DMD Fast Forward. Published on July 9, 2009 as doi:10.1124/dmd.108.025759

24-Hydroxycholesterol Sulfation by Human Cytosolic Sulfotransferases: Formation of Monosulfates and Disulfates, Molecular Modeling, Sulfatase Sensitivity and Inhibition of LXR Activation

Ian T. Cook, Zofia Duniec-Dmuchowski, Thomas A. Kocarek, Melissa Runge-Morris and Charles N. Falany

Department of Pharmacology and Toxicology, University of Alabama at Birmingham, Birmingham, AL, 35294 (ITC, CNF); Institute of Environmental Health Sciences, Wayne State University, Detroit, MI, 48201(ZD-D, TAK, MR-M)

DMD Fast Forward. Published on July 9, 2009 as DOI: 10.1124/dmd.108.025759
This article has not been copyedited and formatted. The final version may differ from this version.

Running title: 24-Hydroxycholesterol conjugation by human SULTs

Corresponding author:

Charles N. Falany, Ph.D.
Dept. of Pharmacology and Toxicology
1670 University Blvd., Volker Hall G133M
University of Alabama at Birmingham Birmingham, AL, USA 35294
Phone: 205-934-9848 Fax: 205-934-9888
E-mail: cfalany@uab.edu

Number of Tables:	1
Number of Figures:	9
Number of References:	41
Number of Words:	
Abstract:	236
Introduction:	679
Discussion:	1785

Abbreviations: 24(S)-Hydroxycholesterol (24-OHChol), 3'-Phosphoadenosine-5'-phosphosulfate (PAPS), sulfotransferase (SULT), liver-X-receptor (LXR), cytochrome P450 (CYP), organic anion transporter (OAT), Steroid sulfatase C (STS), Time-resolved fluorescence resonance energy transfer (TR-FRET), apolipoprotein E (Apo E)

DMD Fast Forward. Published on July 9, 2009 as DOI: 10.1124/dmd.108.025759
This article has not been copyedited and formatted. The final version may differ from this version.

ABSTRACT

24-Hydroxycholesterol (24-OHChol) is a major cholesterol metabolite and the form in which cholesterol is secreted from the brain. 24-OHChol is transported by apolipoprotein E to the liver and converted into bile acids or excreted. In both brain and liver, 24-OHChol is a liver-X-receptor (LXR) agonist and has an important role in cholesterol homeostasis. 24-OHChol sulfation was examined to understand its role in 24-OHChol metabolism and its effect on LXR activation. 24-OHChol was conjugated by three isoforms of human cytosolic sulfotransferase (SULT). SULTs 2A1 and 1E1 sulfated both the 3- and 24-hydroxyls to form the 24-OHChol-3, 24-disulfate. SULT2B1b formed only 24-OHChol-3-sulfate. The 3-sulfate as a monosulfate or as the disulfate was hydrolyzed by human placental steroid sulfatase, whereas the 24-sulfate was resistant. At physiological 24-OHChol concentrations, SULT2A1 formed the 3-monosulfate and the 3, 24-disulfate due to a high affinity for sulfation of the 3-OH in 24-OHChol-24-sulfate. Molecular docking simulations indicate that 24-OHChol-24-sulfate binds in an active configuration in the SULT2A1 substrate binding site with high affinity only when the SULT2A1 homodimer structure was utilized. 24-OHChol is an LXR activator. In contrast, the 24-OHChol monosulfates were not LXR agonists in a FRET-coactivator recruitment assay. However, both the 24-OHChol-3-sulfate and 24-sulfate were antagonists of LXR activation by T0901317 with IC50s of 0.15 and 0.31 μM, respectively. Inhibition of LXR activation by the 24-OHChol monosulfates at low nanomolar concentrations indicates that sulfation has a role in LXR regulation by oxysterols.

DMD Fast Forward. Published on July 9, 2009 as DOI: 10.1124/dmd.108.025759
This article has not been copyedited and formatted. The final version may differ from this version.

INTRODUCTION

24(S)-Hydroxycholesterol (24-OHChol) is the major metabolite of cholesterol in human brain and the form in which cholesterol is secreted across the blood brain barrier (Bjorkhem et al., 1998; Mast et al., 2003). Regulation of cholesterol levels in the brain is vital in maintaining proper neuronal activity. 24-OHChol is synthesized by the brain specific cytochrome P450 (CYP) 46A isoform and is transported out of the brain by the organic anion transporter (OAT)-2 (Bjorkhem 2006). It is subsequently carried in the circulation by apolipoprotein (Apo) E to the liver where it can be hydroxylated by CYP7A and converted into bile acids (Bjorkhem, 2001; Fujiyoshi et al. 2007). However, conversion to bile acids accounts for only 40-50% of 24-OHChol elimination leaving a large fraction of 24-OHChol metabolism and excretion unresolved (Bjorkhem, 2001). Conjugation with either sulfonate or glucuronic acid has been implicated as important for biliary excretion (Bjorkhem, 2001).

Although 24-OHChol represents a mechanism for cholesterol secretion in the CNS, it also has a role in the regulation of cholesterol mobilization. Several oxysterols including 24-OHChol, are endogenous ligands for activation of the liver-X-receptors (LXRs) (Janowski et al., 1999). In brain, activation of LXRß by 24-OHChol is associated with increased mobilization of cholesterol for use in myelin formation and synaptic plasticity (Koudinov et al., 2008). LXRß activation also induces expression of OAT-2 and ApoE that are involved in the increased secretion of 24-OHChol from the brain and its transport to the liver (Bjorkhem et al., 1998). In rats, LXRα activation reportedly results in the induction of hepatic CYP7A leading to increased 7α-hydroxylation of 24-OHChol and its conversion into bile acids (Lehmann et al., 1997); however, CYP7A1 expression may not be induced in human hepatocytes (Chen et al., 2002). Although oxysterols may activate LXRs, the ability of 24-OHChol-monosulfates or the 3-, 24-disulfate to either activate or inhibit LXR has not been reported.

Sulfation of oxysterols and 24-OHChol by selected isoforms of human cytosolic sulfotransferase (SULT) has recently been reported (Javitt et al., 2001; Fuda et al., 2007). Sulfation involves the transfer of the sulfonate group of the obligate sulfonate donor 3'-phosphoadenosine-5'-phosphosulfate (PAPS) to an acceptor compound, usually possessing a hydroxyl group, to form a sulfate ester. The reaction is catalyzed by a family of cytosolic SULTs involved with the conjugation of therapeutic drugs, xenobiotics and small endogenous compounds including hydroxysteroids, thyroid hormones, estrogens, bile acids, cholesterol and oxysterols (Falany,

1997; Glatt et al., 2000). The isoforms of human SULT responsible for the formation of 24-OHChol monosulfates and disulfate as well as the kinetics of these reactions have not been well described.

Conjugation of a compound with a sulfonate group is generally considered to be an inactivation reaction. However, the parent compound can in many cases be regenerated by hydrolysis by sulfatase activity (Iwamori, 2005). Steroid sulfatase C (STS) is expressed in human liver and is responsible for the hydrolysis of many estrogen and hydroxysteroid sulfates including dehydroepiandrosterone (DHEA)-sulfate and ß-estradiol (E2)-3-sulfate (Iwamori, 2005; Hernandez-Guzman et al., 2001). However, the sulfates of some hormonally active drugs are resistant to STS. The 3α-sulfate of tibolone is resistant to STS whereas the 3ß-sulfate of tibolone is hydrolyzed (Falany and Falany, 2007). Also, the benzothiophene sulfate of raloxifene is hydrolyzed by STS whereas the phenolic sulfate of raloxifene is resistant (Falany and Falany, 2007). The sensitivity of the 24-OHChol monosulfates and disulfate to STS has not been reported. Selective hydrolysis of the 3- or 24-sulfates could lead to the formation and accumulation of selective 24-OHChol metabolites.

In this report, the major SULT isoforms responsible for the formation of the 24-OHChol monosulfates and disulfate are identified. The kinetic properties of the reactions are described as well as the molecular docking of 24-OHChol and the monosulfates in the active sites of SULT2A1 to better understand the mechanism by which the different sulfated products are generated. 24-OHChol-24-sulfate, which is rapidly converted to the 3, 24-disulfate, can only be modeled in an apparently active configuration when the published SULT2A1 homodimer structure was used (PDB 1EFH). Sensitivity of the 24-OHChol sulfates to hydrolysis by STS is described. The 24-OHChol monosulfates were not LXR activators; however, the ability of the 24-OHChol monosulfates to inhibit activation of LXRα at physiologically relevant concentrations was demonstrated. This information is important for developing a better understanding of the metabolism as well as the role activity of 24-OHChol and its sulfated metabolites in the regulation of LXR activation.

DMD Fast Forward. Published on July 9, 2009 as DOI: 10.1124/dmd.108.025759
This article has not been copyedited and formatted. The final version may differ from this version.

MATERIALS

24-OHChol was purchased from BioMol (Plymouth Meeting, PA). LK6DF 60 Å silica gel thin-layer chromatography (TLC) plates with a layer thickness of 250 µm were obtained from Whatman Inc. (Clifton, NJ). PAPS was purchased from Dr. Sanford Singer (University of Dayton, Dayton, OH). [^{35}S]PAPS (2.2 Ci/mmol) and [1,2,6,7-^{3}H(N)]DHEA-sulfate (60 Ci/mmol) were purchased from New England Nuclear. C-18 Sep-Pak cartridges were purchased from Waters. The pQE-31 vector and Ni-NTA resin were purchased from Qiagen (Valencia, CA). Con A Sepharose and DEAE-Sepharose Cl-6B were from GE Healthcare (Pittsburgh, PA). T0901317 (N-(2,2,2-trifluoroethyl)-N-[4-[2,2,2-trifluoro-1-hydroxy-1-(trifluoromethyl)ethyl]phenyl]-benzenesulfonamide) was obtained from Sigma (St. Louis, MO). The LanthaScreen TR-FRET LXRα Coactivator Assay kit was from Invitrogen (Carlsbad, CA). All other materials were purchased from Fisher Scientific (Norcross, GA).

METHODS

Preparation of SULT isoforms and STS -The native forms of SULT1E1 and SULT2A1 were expressed in *E. coli* DH5α and purified by DEAE-Sepharose Cl-6B chromatography as described previously (Falany et al., 1994). The amount of the individual SULT isoforms in the preparations were estimated by comparison to known standards during immunoblot analysis.

Since SULT2B1b cannot be expressed in an active native form in *E. coli* (Meloche and Falany, 2001; Falany et al. 2006), the enzyme was subcloned into pQE-31 and expressed in *E. coli* DH5α with a cleavable 6xHis-tag. The expressed His-SULT2B1b protein was purified on a Ni–NTA affinity column. To recover native SULT2B1b, the His-tag was cleaved by rTev protease and the preparation passed through the Ni-NTA affinity column again to remove the His-tag from the pure SULT2B1b. This generated an active but relatively unstable preparation of native SULT2B1b (Meloche and Falany, 2001; Falany et al. 2006).

STS was purified from human full-term placenta using the method of Hernandez-Guzman *et al*. (2001) as described previously (Falany and Falany, 2007). Briefly, fresh term human placental tissue was obtained from the Tissue Procurement Service of the UAB Comprehensive Cancer Center. The placental tissue was homogenized in 67 mM phosphate buffer, pH 7.4 containing 0.5 mM DTT and 0.24 M sucrose and stored at -80°C until use. For STS purification, placental

homogenate was thawed on ice and diluted with 10mM potassium phosphate, pH 7.4, 20% glycerol, 0.5 µM androstenedione and 0.1 mM EDTA, then centrifuged at 105,000 x *g* for 60 min. The pellet was then homogenized in the same buffer, adjusted to 0.3% Na cholate and 0.3% Emulgen 911, stirred at 4°C for 30 min, then centrifuged at 105,000 x g for 1 h. The supernatant fraction was diluted with an equal volume of the same buffer then loaded on a 60 ml DE-52 anion-exchange column equilibrated in the same buffer. The column was washed with buffer containing 0.15% Emulgen 911 then with 20 mM Tris–HCl, pH 7.4 containing 0.1% Triton X-100. STS activity was then eluted with 0.15 M NaCl in the same buffer in 3 ml fractions. Fractions containing STS activity were pooled and adjusted to contain 5 mM $CaCl_2$, 5 mM $MgCl_2$, 5 mM $MnCl_2$ and 1 M NaCl. The pool was stirred for 30 min at 4°C then centrifuged at 105,000 x g for 30 min. STS was further purified from the supernatant fraction on a 5 ml Con-A Sepharose column equilibrated in 20 mM Tris-HCl, pH 7.4, containing 0.1% Triton X-100, 5 mM $CaCl_2$, 5 mM $MgCl_2$, 5 mM $MnCl_2$ and 1 M NaCl. Subsequent to the wash step, STS was eluted with 10% αmannopyranoside and fractions containing STS activity were pooled. The α-mannopyranoside was removed by repeated concentration and dilution using a Centricon 30,000 MWCO membrane. The purified STS was aliquotted and stored at -80°C.

SULT and STS Assays – 24-OHChol sulfation assays were carried out using a standard procedure for the sulfation of non-radiolabeled sulfonate acceptor substrates (Meloche and Falany, 2001). In brief, reactions contained 75 mM Tris-HCl, pH 7.4, 5 mM $MgCl_2$ buffer and either 24-OHChol in ethanol or an equal volume of ethanol alone. Enzyme was added to the mixture and equilibrated for 2 min at 37°C. [^{35}S]PAPS was then added to the mixture to start the reaction. The reactions were terminated by chloroform extraction and the sulfated products in the aqueous phase resolved by thin layer chromatography (TLC) on silica gel TLC plates using a solvent system of methylene chloride, methanol and ammonium hydroxide (84:16:5). The plates were dried and exposed to autoradiograph film then the radioactive spots scraped for quantitation by scintillation counting.

To determine the sensitivity of the 24-OHChol sulfates to STS hydrolysis, the 24-OHChol-3-sulfate was generated using SULT2B1b and the 24-OHChol-3-monosulfate and disulfate were synthesized with SULTs 2A1 and 1E1. The reactions were terminated by chloroform extraction and the aqueous phase containing the sulfates divided into two fractions. One fraction was analyzed by TLC for quantification of 24-OHChol sulfation. The other fraction was incubated at 37°C for 2 min to vaporize the residual chloroform, then 0.5 µg of purified STS was added and

the reaction incubated for 15 min. After hydrolysis of the 24-OHChol sulfates with STS, the products were analyzed by TLC and autoradiography.

STS activity was determined using reactions containing 20 uM [^{3}H]DHEA-sulfate as substrate in 0.1 M Tris–maleate buffer, pH 7.4. STS was added to start the reaction and the reactions were stopped by the addition of 0.25 M Tris–HCl, pH 8.7 to alkalinize the reaction followed by extraction with chloroform. Radioactivity was determined in an aliquot of the chloroform phase by scintillation counting to quantify the generation of desulfated [^{3}H]DHEA.

Molecular Docking Simulations - For the molecular simulations of the docking of 24-OHChol and its sulfates into the substrate binding sites of SULT2A1, the 24-OHChol PDB file was generated from a cholesterol PDB file (1LRI) (Lascombe et al., 2002) and an OH moiety was added manually at the 24-position. The 24-OHChol sulfates were generated by the addition of the appropriate sulfonates and the structures energetically minimized with Autodock (Scripps Research Inst.). The crystal structure used for the docking studies was SULT2A1 solved with PAP in the binding site (PDB file 1EFH) (Pedersen et al., 2000). A SULT2A1 structure solved with DHEA in the binding site (PDB file 1J99) was used for initial orientation of the hydroxyl groups of the 24-OHChol compounds (Rehse et al., 2002). The positioning of either of the nucleophilic hydroxyl groups of 24-OHChol and the sulfated metabolites was based on the position of the 3-hydroxyl of DHEA. Protons were added to the structure (pH 7), and electrostatic potentials and charges were assigned by Autodock that includes terms for sulfur and phosphorus. An energetically minimized configuration was calculated for each of the 24-OHChol models with Autodock (Huey et al., 2007) using a Lamarckian search with a population of 150 initial test orientations and a minimum of 2.5 x 10^6 iterations. The binding free energy (BFE) was calculated for the lowest energy configuration.

Mass Spectroscopy - To identify 24-OHChol and the sulfated reaction products, nonradioactive reactions were run in parallel with reactions containing [^{35}S]PAPS that were monitored by TLC. The non-radioactive reactions were extracted with chloroform and the water phase loaded onto a Sep-Pak cartridge, washed with water and eluted with MeOH. The eluates were concentrated by evaporation under a stream of N_2. Identification of the 24-OHChol mono-and disulfates was carried out by HPLC-mass spectroscopy using a Sciex API-4000 Triple Quadrupole mass spectrometer with two Perkin Elmer series 200 micropumps (Perkin Elmer Life and Analytical Sciences, Boston, MA) and a Synergi Fusion (100 x 2 mm ID) analytical C-18 column with a C-

DMD Fast Forward. Published on July 9, 2009 as DOI: 10.1124/dmd.108.025759
This article has not been copyedited and formatted. The final version may differ from this version.

18 guard column (Phenomenex). The mobile phases were: A, 10 mM ammonium acetate; and B, 100% acetonitrile/10 mM ammonium acetate. The gradient profile was 0 to 5 min, 100% A; 5 to 10 min, 20% A (linear); 10 to 15 min 20% A; and 15 to 20 min 100% A (step). Mass spectroscopy results were analyzed with the Analyst 1.4 software (Applied Biosystems, Foster City, CA). Identification of the 24-OHChol-monosulfates and disulfate was carried out by MS/MS to generate the parent 24-OHChol and sulfate ions. MS/MS analysis of the putative 24-OHChol-monosulfates was attempted with increasing collision energies (30-120eV). Fragmentation other than the parent and sulfate ions was observed only with the 24-OHChol-24-monosulfate.

Time-resolved fluorescence resonance energy transfer (TR-FRET) LXRα coactivator recruitment assay. A sample of 25 µM 24-OHChol-3-sulfate in ethanol was evaporated under nitrogen and re-dissolved in DMSO to a concentration of 250 µM. A sample of 5 µM 24-OHChol-24-sulfate in 50% ethanol was evaporated under nitrogen and re-dissolved in DMSO-methanol (50:50) to a concentration of 50 µM. Then 1:2 dilutions of each sterol sulfate were prepared in DMSO. The synthetic LXR agonist, T0901317 (dissolved in DMSO), and the parental oxysterol, 24-OHChol (dissolved in ethanol), were included as positive control LXR ligands. The LanthaScreen TR-FRET LXRα Coactivator Assay was used according to the manufacturer's instructions (Invitrogen). To test the ability of an agent to bind to LXRα as an agonist, a dilution series was prepared at 100X and then diluted to 2X with Complete TR-FRET Coregulator Buffer H. A 10 µl aliquot of each dilution was transferred to the wells of a 384-well plate in triplicate, and 5 µl 20nMLXRα-ligand-binding domain was added to each well followed by 5 µl of a mixture containing 1 µM fluorescein-labeled TRAP220/DRIP-2 peptide and 40 nM terbium-conjugated anti-glutathione S-transferase antibody. The plate was sealed, protected from light and incubated with gentle shaking for 2 h at room temperature and read with a Victor^3 Multilabel Reader (PerkinElmer), with an excitation wavelength of 340 nm, emission wavelengths of 520 and 490 nm, a delay time of 100 µs and an integration time of 200 µs. Emission ratios were calculated as the quotients of the emission values at 520 nm divided by the emission values at 490 nm. Binding curves were generated using the log(agonist) vs. response-variable slope function of Prism 5 (GraphPad). To test the ability of an agent to bind to LXRα as an antagonist, assays were performed as described above, except that each binding reaction also contained 100 nM T0901317, and binding curves were generated using the log(inhibitor) vs. response-variable slope function of Prism 5.

DMD Fast Forward. Published on July 9, 2009 as DOI: 10.1124/dmd.108.025759
This article has not been copyedited and formatted. The final version may differ from this version.

RESULTS

24-OHChol Sulfation - Seven isoforms of human SULT were tested for their ability to sulfate 24-OHChol including SULTs 1A1, 1A3, 1B1, 1C1, 1E1, 2A1 and 2B1b. Three of the SULT isoforms were capable of sulfating 24-OHChol (SULTs 1E1, 2A1, 2B1b) whereas the other isoforms displayed no detectable activity. Figure 1 shows that SULT2A1 was capable of forming both 24-OHChol monosulfates as well as the 3, 24-disulfate, whereas SULT2B1b formed only a 24-OHChol monosulfate. SULT1E1 was also capable of forming both 24-OHChol monosulfates and the disulfate (supplemental data).

Hydrolysis by STS – The sensitivity of the different 24-OHChol sulfates to hydrolysis by placental STS was examined. Figure 1 also shows that the single 24-OHChol-monosulfate formed by SULT2B1b was completely hydrolyzed by STS treatment. In contrast, the 3, 24-disulfate formed by SULT2A1 was hydrolyzed to a STS-resistant monosulfate. Therefore, SULT2B1b formed a single 24-OHChol-monosulfate that was sensitive to STS hydrolysis, whereas, in the disulfate formed by SULT2A1 only one of the possible monosulfates was cleaved. The remaining STS-resistant monosulfate indicated that the monosulfate formed by SULT2B1b and the STS-sensitive monosulfate synthesized by SULT2A1 were identical.

24-OHChol sulfation by SULT2A1 – Figure 2A shows that at low 24-OHChol concentrations the overall rate of disulfate formation was more rapid than monosulfate formation. To understand the mechanism for the rapid 3, 24-disulfate synthesis, the rates of monosulfate and disulfate formation were examined. Figure 2B shows the relationship between the formation of 24-OHChol-monosulfates and disulfate, and their sensitivity to STS hydrolysis. Treatment of the sulfated products with STS resulted in the formation of a STS-resistant monosulfate in equal amounts to the amount of disulfate present in the initial reaction. This data indicates that the monosulfate present in the reaction mixture was sensitive to STS hydrolysis, whereas, the disulfate is being hydrolyzed to a STS-resistant monosulfate. Very little of the STS-resistant monosulfate was present in the reaction mixture before STS treatment.

24-OHChol sulfation by SULT1E1 – SULT1E1 was also capable of forming detectable amounts of 24-OHChol disulfate although at significantly lower rates than SULT2A1 (Fig. 3). In contrast to SULT2A1, SULT1E1 formed primarily monosulfates at low 24-OHChol concentrations. The amount of 24-OHChol-disulfate generated in these reactions was approximately 20% of the

monosulfate formed. At concentrations above 7 μM 24-OHChol-monosulfate formation showed apparent substrate inhibition, a feature frequently observed with the SULTs (Falany et al., 1994; Zhang et al., 1998). The major monosulfate formed by SULT1E1 was also sensitive to hydrolysis by STS. Very little of the STS-resistant monosulfate was present in the initial reaction since the amounts of STS-resistant monosulfate present after STS treatment are similar to the levels of 24-OHChol-disulfate present in the initial reaction (Fig. 3).

24-OHChol sulfation by SULT2B1b – Of the three SULT isoforms capable of sulfating 24-OHChol, SULT2B1b was the only isoform that formed only 24-OHChol-monosulfates. Figure 4 shows that SULT2B1b required higher 24-OHChol concentrations for activity as compared to SULTs 1E1 and 2A1 although the rates of sulfation were also generally greater. Figure 1 also demonstrates that the single 24-OHChol-monosulfate formed by SULT2B1b is the STS-sensitive monosulfate.

LC MS/MS analysis of the sulfation of 24-OHChol – The sulfation of 24-OHChol by SULTs 2A1 and 2B1b was analyzed by LC-MS/MS to identify the monosulfates and the products of STS hydrolysis. Figure 5A shows the elution of the 24-OHChol-monosulfates generated by SULT2A1. The major peak eluting at 9.0 min is the 3-monosulfate and the smaller peak at 8.3 min is the 24-monosulfate. Treatment of the initial reaction products with STS resulted in the total loss of only the 9.0 min or 3-monosulfate peak. This is consistent with the selectivity of STS for the hydrolysis of 3ß-sulfates as compared to 3α-sulfates on steroidal compounds (Falany and Falany, 2007). Figure 5B shows the elution of the 24-OHChol-3, 24-disulfate formed by SULT2A1. Hydrolysis of the disulfate with STS generated only the 8.3 min or 24-monosulfate peak (Fig. 5C) indicating that 24OHChol-24-sulfate is the STS-resistant monosulfate. Figure 5D demonstrates that SULT2B1b formed only the 3-monosulfate and was apparently incapable of forming either the 24-sulfate or the disulfate consistent with the selectivity of SULT2B1b for conjugation of 3ß-hydroxysteroids (Falany et al., 2006). The 24-OHChol-3-monosulfate formed by SULT2B1b was also completely hydrolyzed by STS.

To define the sites of sulfate conjugation an LC-MS/MS approach was utilized. The analysis was complicated by the tendency for the loss of the sulfate group before fragmentation of the ring system. Utilizing a range of eV potentials for the fragmentation of the putative 24-OHChol-24-sulfate molecule generated a fragment possessing the 3ß-OH moiety and portions of the A ring (Fig. 6). This is consistent with sulfate conjugation at the 24-position supporting its identity

DMD Fast Forward. Published on July 9, 2009 as DOI: 10.1124/dmd.108.025759
This article has not been copyedited and formatted. The final version may differ from this version.

as 24-OHChol-24-sulfate. LC-MS/MS analysis of the putative 24-OHChol-3-sulfate under similar conditions generated only the parent and sulfate ions. However, the LC-MS/MS identification of the 24-OHChol-24-sulfate and 24-OHChol-3-sulfate are consistent with their anticipated STS sensitivities and expected syntheses especially the formation of the 3-monosulfate by SULT2B1b that is highly selective for the sulfation of 3ß-hydroxysteroids (Meloche and Falany, 2001).

Metabolism of the 24-OHChol monosulfates to the disulfate by SULT2A1 – Analysis of the products of the sulfation of 24-OHChol by SULT2A1 indicates that the major products formed are the 3-monosulfate and the disulfate. Very little of the 24-monosulfate was detected (Fig. 5). To examine whether one of the monosulfates was the preferred substrate for conversion to the disulfate, both of the 24-OHChol monosulfates were purified and used in assays with SULT2A1 to form the disulfate. Figure 7 shows the effect of increasing concentrations of the separate monosulfates on their conversion to 24-OHChol disulfate. The conversion of the 24-sulfate to the disulfate occurs at much lower concentrations and with a higher rate than sulfation of the 3-monosulfate.

Kinetics of 24-OHChol sulfation – Table 1 presents the kinetic parameters determined for the formation of the different sulfated metabolites of 24-OHChol catalyzed by SULTs 2A1, 1E1 and 2B1b. SULT2B1b demonstrated the highest Km (23.5 µM) and a Kcat of 218 min^{-1} for the formation of 24-OHChol-3-sulfate, its only product. SULT1E1 had a Km of 0.9 µM for the synthesis of the 3-monosulfate with a Kcat of 55 min^{-1}. For the overall metabolism of 24-OHChol to a disulfate, SULT1E1 had a relatively high Km of 4.9 µM and the lowest Kcat (4 min^{-1}) of the reactions analyzed. SULT2A1 showed a Km of 3.7 µM for the synthesis of the 3-monosulfate with a Kcat equivalent to that of SULT2B1b (218^{-1}). The overall conversion of 24-OHChol to the disulfate by SULT2A1 had a Km of 1.5 µM and a Kcat of 133 min^{-1}, consistent with the favored formation of the disulfate by SULT2A1 at low 24-OHChol concentrations.

The detection of low amounts of 24-OHChol-24-monosulfate during the sulfation of 24-OHChol by SULT2A1 suggested that the 24-monosulfate was more rapidly converted to the disulfate than the 3-monosulfate. Table 1 shows that the Km for the conversion of 24-OHChol-24-sulfate to the disulfate by SULT2A1 was 0.1 µM and the Kcat is 2410 min^{-1}, whereas the conversion of the 3-sulfate to the disulfate possessed a 40-fold higher Km and 20-fold lower Kcat. These data indicate that SULT2A1 forms both 24-OHChol monosulfates at low concentrations, however,

DMD Fast Forward. Published on July 9, 2009 as DOI: 10.1124/dmd.108.025759
This article has not been copyedited and formatted. The final version may differ from this version.

because of its higher affinity the 24-monosulfate is rapidly converted to the disulfate. Therefore, the Km and Vmax for the overall conversion of 24-OHChol to the disulfate are a good estimate for the formation of the 24-monosulfate.

Molecular modeling of the 24-OHChol monosulfates in the active site of SULT2A1 – The sulfation of 24-OHChol results in the formation of the 3-monosulfate and the 3, 24-disulfate. Lack of detection of the 24-monosulfate in the reactions was apparently due to the high affinity of the 24-monosulfate for conversion to the disulfate (Table 1). To examine the molecular interactions associated with the rapid formation of 24-OHChol disulfate, both the 24-OHChol-monosulfates were docked in the active site of SULT2A1. First, the affinity of 24-OHChol with either the 3-hydroxyl or 24-hydroxyl positioned for catalysis in the substrate binding site of SULT2A1 was analyzed using Autodock. The BFE of 24-OHChol with either the 3-hydroxyl or 24-hydroxyl in the active site was -6.0 and -6.1 kcal/mol, respectively, indicating a similar affinity for sulfation at both hydroxyls. The non-sulfated hydroxyl groups of both compounds were positioned appropriately in relation to PAP and the active site His99 residue for catalysis. The first three preferred binding orientations for sulfation of both the 3-OH and 24-OH positions in 24-OHChol and the second and third preferred orientations for both the 24-OHChol monosulfates are included as Supplemental Data.

The conjugation of compounds with a bulky charged sulfonate group generally limits their further metabolism. To assess the mechanism for the high affinity of 24-OHChol-24-sulfate for sulfation to the 3, 24-disulfate, the binding of both the 3- and 24-monosulfates in the active site of SULT2A1 was analyzed. Figure 8A depicts the optimal orientation of 24-OHChol-3-sulfate in the binding pocket of SULT2A1 using the Autodock program to minimize the BFE. 24-OHChol3-sulfate orients in the binding pocket of SULT2A1 in association with PAP and the active site His99 residue with a BFE of -3.5 Kcal/mol. In contrast, 24-OHChol-24-sulfate did not bind in the substrate binding pocket in a catalytically competent orientation when the docking experiment utilized the SULT2A1 monomer structure. Figure 8B shows the optimal binding orientation of the 24-OHChol-24-sulfate in the SULT2A1 monomer. The 24-sulfate group strongly interacts with Lys138 and the 3-hydroxyl group hydrogen bonds with Ser80 preventing entry of 24-OHChol-24-sulfate into the binding pocket. The BFE of this orientation is -10.0 Kcal/mol. The 3-OH group of 24-OHChol-24-sulfate is positioned approximately 9 Angstroms from the active site His99 residue. Since the BFE and orientation of the 24-sulfate in the substrate binding pocket of SULT2A1 are inconsistent with the high affinity and reactivity of the 24-sulfate to the disulfate

observed in the kinetic experiments, the docking experiments were carried out using the dimer structure of SULT2A1 (PDB file 1EFH). Figure 8C demonstrates that when using the homodimer structure of SULT2A1, 24-OHChol-24-sulfate orients in the binding pocket with the 3-hydroxyl group in a position close to PAP and the active site His99 residue consistent with efficient catalysis. The BFE is -7.9 Kcal/mol indicating that the 24-OHChol-24-sulfate is a better substrate for a second sulfation and conversion to a disulfate than the 3-monosulfate. The ability of 24-OHChol-24-sulfate to efficiently bind with the 3-hydroxyl in a catalytically competent orientation results from an interaction of Glu73 from the second SULT2A1 molecule in the homodimer structure blocking access for the 24-sulfate group of 24-OHChol-24-sulfate to interact with Lys138. Since the 24-sulfate moiety cannot bind to Lys138 in the SULT2A1 homodimer due to the presence of the Glu73 residue, the 24-OHChol-24-sulfate can enter into the binding pocket and situate closer to PAP and the His99 residue.

Agonist and antagonist properties of the 24-OHChol sulfates in the activation of LXRα - Oxysterols including 24-OHChol, are considered physiological agonists of the LXRs (Jankowski et al., 1999); Lehman et al., 1997). To test for interaction of 24-OHChol and its sulfated metabolites with LXRα, a FRET-based coactivator recruitment assay was used. Figure 9A indicates that the synthetic LXR agonist T0901317 and 24-OHChol were capable of activating LXRα with EC50s of 0.30 μM and 1.99 μM, respectively. Both 24-OHChol-3-sulfate and the 24-sulfate were tested for LXR activation activity and no ability to activate LXRα was observed. Although neither 24-OHChol-monosulfates activated LXRα, both monosulfates were tested for their ability to antagonize the activation activity of T090137. Figure 9B shows that both 24-OHChol monosulfates were efficient antagonists of LXRα activation by 100 nM T0901317. The IC50s of 24-OHChol-3-sulfate and 24-sulfate were 0.15 and 0.31 μM, respectively, indicating that the monosulfates were better inhibitors of LXR activation in the coactivator assay than the parent 24-OHChol was an agonist.

DMD Fast Forward. Published on July 9, 2009 as DOI: 10.1124/dmd.108.025759
This article has not been copyedited and formatted. The final version may differ from this version.

DISCUSSION

Synthesis of 24-OHChol is the major mechanism for the removal of cholesterol from the brain and after transport to the liver it is a substrate for the synthesis of bile acids (Bjorkhem, 2006; Bjorkhem et al., 2001). As an oxysterol, 24-OHChol is also considered an important mediator of the activity of nuclear receptors including the LXRs (Lehman et al., 1997). In brain, 24-OHChol is synthesized by CYP46 (Mast et al., 2003) and acts to increase cholesterol mobilization for membrane synthesis and synaptic remodeling via LXRß activation (Cartagena et al., 2008). LXR activation also induces OAT-2 and ApoE synthesis resulting in the transport of 24-OHChol from the brain into the circulation (Abildayeva et al., 2006). 24-OHChol circulates bound to ApoE and is taken up by the liver for metabolism and excretion. In liver and macrophages, 24-OHChol is involved in the activation of LXRα and stimulates reverse cholesterol transport and the retention of fatty acids (Naik et al., 2006; Calpe-Berdiel et al., 2008).

24-OHChol is synthesized in neurons in the CNS, secreted from brain and carried to the liver. In the liver, approximately 50% of the 24OHChol is converted to bile acids following 7α-hydroxylation catalyzed by either CYP 39 or CYP7A (Bjorkhem et al., 2001; Bjorkhem, 2007). Bjorkhem et al. (2001) reported that 24-OHChol is also secreted in the bile as sulfate and glucuronide conjugates and that sulfate/glucuronide diconjugates are also formed. In Ileocecal fluid from patients, sulfates represented 3 – 45% of the 24-OHChol detected while 40 - 50% was present as glucuronide conjugates although this fraction included the sulfate/glucuronide diconjugates. The relative positions of the sulfates and glucuronides in the diconjugate were not reported. These authors did not detect the presence of 24-OHChol disulfates that are formed at low 24-OHChol concentrations by SULT2A1 which is one of the two most abundant SULT isoforms in human liver (Falany, 1997; Glatt et al., 2000). Sulfated 24-OHChol has been detected in the brain and in the circulation. Considerable amounts of 5-cholestene-3β,24S,27-triol were also detected in Ileocecal fluid suggesting the hydroxylation of 24-OHChol by CYP27 and this metabolite was also readily conjugated (Bjorkhem, 2007). Therefore, sulfation represents a major pathway for the metabolism of 24-OHChol in the brain, circulation and liver although many of the details of the metabolism of 24-OHChol in different human tissues remain to be identified.

Of the major SULT isoforms tested, only three showed activity in sulfating 24-OHChol, SULTs 2A1, 1E1 and 2B1b. These are the major isoforms associated with steroid sulfation in human

tissues. Consistent with its selective activity in conjugating 3ß-hydroxysteroids (Falany et al., 2006), SULT2B1b formed only 24-OHChol-3-monosulfates although with the lowest affinity and highest Vmax of the three isoforms (Table 1). SULT2B1b also readily sulfates cholesterol (Javitt et al., 2001) and in human keratinocytes the expression of SULT2B1 was inducible by LXR activation (Jiang et al., 2005). SULT2B1b is widely expressed in human tissues including brain, although its expression was not detectable in liver (Falany et al., 2006; Geese and Raftogianis, 2001). The regulation of SULT2B1b expression in brain tissues by LXR activation has not been described.

Identificaton of the 24-OHChol-monosulfates was accomplished using several methods. LC-MS/MS was used to identify the 24-OHChol monosulfates and disulfate by selective ion-monitoring and loss of the sulfate moieties. The monosulfates also demonstrated different elution times. The 3-sulfate was assigned by its sensitivity to STS hydrolysis that is specific for the 3-position of sterols (Iwamori, 2005; Hernandez-Guzman et al., 2001; Falany and Falany, 2007), differential formation by SULT2A1 and 2B1b; SULT2B1b is highly selective for the 3-position of sterols, and docking affinities of 24-OHChol in the active sites of SULT2A1 and 2B1b. Both the 3-OH and 24-OH positions orient in the active site of SULT2A1 in apparently catalytically active orientations (Supplemental Fig.s 1, 2), whereas in SULT2B1b only the 3-OH of 24-OHChol is positioned in an active configuration (Supplemental Fig. 6). These approaches are consistent with SULT2A1 conjugating both hydroxyls and SULT2B1b forming only the 3-sulfate. Identification of 24-OHChol-monosulfate was achieved by MS/MS analysis via detection of a fragment containing the 3-OH moiety (Fig. 6). In contrast, MS/MS analysis of the putative 24-OHChol-3-monosulfate only gave rise to the parent 24-OHChol and sulfate ions.

SULT1E1 has a Km for E2 sulfation of 4 nM and is an important mechanism for the inactivation of E2 in human tissues (Zhang et al., 1998; Kotov et al., 1999). SULT1E1 also sulfates hydroxysteroids (Falany et al., 1994; Falany et al., 1995) although with an affinity similar to that for the formation of 24-OHChol-3-sulfate (Table 1). SULT1E1 displayed a low rate of 24-OHChol-disulfate formation indicating that the 24-hydroxyl of 24-OHChol was not an efficient site for sulfation. Similar to SULT2B1b, SULT1E1 displayed a strong preference for the formation of the 3-monosulfate although with a better affinity but lower activity. SULT1E1 is not as widely expressed in tissues as SULT2B1b being detected primarily in estrogen-responsive tissues, although low levels are present in liver (Daunmu et al., 2006)

SULT2A1 is the major SULT expressed in liver and has a relatively broad substrate reactivity being capable of conjugating 3α- and 3ß-hydroxysteroids, estrogens and aliphatic hydroxyls in xenobiotics (Falany et al. 2005). It is capable of conjugating the D-ring hydroxyls of androgens as well as therapeutic drugs such as tibolone (Falany et al., 2004). At low 24-OHChol concentrations that represent physiological levels, SULT2A1 forms approximately equal amounts of the 3-sulfate and the 3, 24-disulfate. Formation of the 3, 24-disulfate results from the high affinity of SULT2A1 for the sulfation of the 3-OH position in 24-OHChol-24-sulfate.

Molecular docking simulations indicate that 24-OHChol has a similar BFE with either the 3-OH or 24-OH groups positioned for efficient catalysis suggesting that both monosulfates are formed at similar rates. Because of the high affinity of SULT2A1 for conjugation of the 3-OH of 24-OHChol-24-sulfate, the 24-sulfate is not readily detected. The 24-OH of 24-OHChol-3-sulfate is not readily conjugated so the 3-sulfate accumulates along with the disulfate. Molecular docking simulations were used to examine the preference of SULT2A1 for sulfation of the 24-sulfate relative to the 3-sulfate. In these studies the 3-sulfate bound similarly in both the SULT2A1 monomer and in the homodimer. In contrast, the 24-sulfate did not bind in the substrate binding pocket when modeled with the SULT2A1 monomer but did orient the 3-hydroxyl properly in the substrate binding pocket when modeled in the SULT2A1 homodimer. The BFE of the 24-OHChol-24-sulfate in the SULT2A1 homodimer was 3.9 Kcal/mol lower than the 3-sulfate consistent with their Km values and the increased metabolism of the 24-sulfate to the 3, 24-disulfate.

The necessity of using the SULT2A1 homodimer (PDB file 1EFH) to obtain a docking orientation with 24-OHChol-24-sulfate that is consistent with its observed sulfation activity supports the previous identification of the dimerization sites in this structure. Petrochenko et al. (2001) have reported that the “KTVE” domain (aa 255-264 in SULT2A1) is the dimerization interface utilized in the SULTs. In contrast, in the SULT2A1 structures the dimerization interface involves amino acids M16-R19, S68-P70, and M228-Y238 (Rehse et al., 2002; Zhou et al., 2001). The reported dimer structure of SULT2A1 (PDB 1EFH) is more consistent with the high affinity sulfation of 24-OHChol-24-sulfate since interaction with Lys138 is blocked by Glu73 in the second SULT2A1 subunit in the homodimer. If the dimerization domain is assumed to be the “KTVE” domain this interaction is not inhibited and 24-OHChol-24-sulfate is not anticipated to be an efficient substrate for conversion to the 3, 24-disulfate. These observations suggest that the different SULT isoforms may utilize different dimerization domains although there is considerable

conservation of structure in the monomeric forms of the enzymes (Allali-Hassani et al., 2007).

Many sulfate esters are sensitive to hydrolysis by STS activity allowing regeneration of the parent compounds in tissues. STS is primarily responsible for the hydrolysis of estrogen sulfates and many hydroxysteroid sulfates including DHEA-3-sulfate. The 3ß-sulfate of 24-OHCol was readily hydrolyzed by STS whereas the 24-sulfate was resistant. Also, in the 3, 24-disulfate only the 3-sulfate was hydrolyzed. Therefore, 3-sulfation of 24-OHChol represents a reversible reaction allowing regeneration of the parent compound by STS activity. Formation of either the 24-sulfate or 3, 24-disulfate is a terminal reaction in that the 24-sulfate is not hydrolyzed. The formation of the stable 24-sulfate will occur primarily in tissues with high levels of SULT2A1 activity such as liver, stomach and the GI tract. Whether sulfation inhibits hydroxylation by CYP7A and conversion into bile acids has not been reported, although this may account for the difference in 24-OHChol synthesis and its conversion into bile acids (Bjorkhem et al., 2001).

Although oxysterols are considered as physiological activators of the LXRs (Jankowski et al., 1999), the properties of the oxysterol sulfates in nuclear receptor activation have not been extensively studied. In the FRET co-activator recruitment assay both of the 24-OHChol monosulfates were significantly better inhibitors of LXR activation than 24-OHChol was an agonist. In human liver that has high levels of SULT2A1 activity, the rapid synthesis of 24-OHChol-3-sulfate and the 3, 24-disulfate would possibly result in the generation of a potent stable LXR antagonist, 24-OHChol-24-sulfate. Liver possesses STS activity indicating that the 3-sulfate in the 3, 24-disulfate may be hydrolyzed regenerating 24-OHChol; however, the 24-sulfate formed from 3, 24-disulfate would be stable due to its resistance to STS hydrolysis. High levels of SULT2A1 activity that favor generation of inhibitory 24-OHChol sulfates are limited to the adrenal cortex, GI tract and liver in humans (Falany et al., 2004). SULT2B1b, that forms only the 3-sulfate is widely expressed in tissues and has been reported to be regulated by LXR in human keratinocytes (Jiang et al., 2005). The induction of SULT2B1b by LXR activation suggests a feedback mechanism by which high levels of 24-OHChol could activate LXR and induce SULT2B1b in tissues such as breast (Dumas et al., 2008) resulting in the increased synthesis of inhibitory 24-OHChol-3-sulfate. STS would then serve to hydrolyze the inhibitory 3-sulfates allowing regeneration of 24-OHChol. In support of the LXR-modulating potential of SULT2B1b-catalyzed oxysterol sulfation, the transactivation of an LXRα reporter gene in HEK293 cells by a naturally occurring oxysterol, 24,25-epoxycholesterol, was substantially impaired by the co-transfection of mouse cholesterol sulfotransferase (SULT2B1b) (Chen et al.,

2007). In addition, when mice were infected with a mouse SULT2B1b adenoviral expression vector, the expression of endogenous LXRα-activated hepatic target genes was decreased. The regulatory properties of the oxysterols and their sulfated metabolites with LXR activation or inhibition in different tissues remains to be elucidated.

The sulfation of 24-OHChol is catalyzed by at least three of the major human cytosolic SULT isoforms with different affinities for the formation of the 24-OHChol monosulfates and disulfate. SULT2B1b forms only the 3-sulfate whereas SULT1E1 forms primarily the 3-sulfate but also a small amount of the 24-sulfate and disulfate. SULT2A1 preferentially catalyzes the formation of the disulfate at relatively low 24-OHChol concentrations due to a high affinity for sulfation of the 24-OHChol-24-sulfate to the disulfate. Only the 3-sulfate was hydrolyzed by human STS allowing for the accumulation of the 24-sulfate in tissues. This may occur primarily in liver due to the abundant expression of SULT2A1. The formation of the 24-OHChol sulfates may be physiologically relevant since both the 24-OHChol monosulfates were 5-6-fold better antagonists of LXR activation than 24-OHChol was an agonist. Elucidating the sulfation of 24-OHChol in human tissues is important for understanding its multiple properties, regulation and metabolism in different human tissues including liver, brain and breast.

REFERENCES

Abildayeva, K., Jansen, P. J., Hirsch-Reinshagen, V., Bloks, V. W., Bakker, A. H., Ramaekers, F. C., de Vente, J., Groen, A. K., Wellington, C. L., Kuipers, F. and Mulder, M. (Falany, 1997; (2006) 24(S)-hydroxycholesterol participates in a liver X receptor-controlled pathway in astrocytes that regulates apolipoprotein E-mediated cholesterol efflux. *J Biol Chem* **281**: 12799-12808.

Allali-Hassani, A., Pan, P. W., Dombrovski, L., Najmanovich, R., Tempel, W., Dong, A., Loppnau, P., Martin, F., Thornton, J., Edwards, A. M., Bochkarev, A., Plotnikov, A. N., Vedadi, M. and Arrowsmith, C. H. (2007) Structural and chemical profiling of the human cytosolic sulfotransferases. *PLoS Biol* **5**: e97.

Bjorkhem, I. (2006) Crossing the barrier: oxysterols as cholesterol transporters and metabolic modulators in the brain. J Intern Med **260**, 493-508.

Bjorkhem, I. (2007) Rediscovery of cerebrosterol. *Lipids* **42**: 5 -14.

Bjorkhem, I., Andersson, U., Ellis, E., Alvelius, G., Ellegard, L., Diczfalusy, U., Sjovall, J and Einarsson, C. (2001) From brain to bile. Evidence that conjugation and omega-hydroxylation are important for elimination of 24S-hydroxycholesterol (cerebrosterol) in humans. *J Biol Chem* **276**: 37004-37010

Bjorkhem, I., Lutjohann, D., Diczfalusy, U., Stahle, L., Ahlborg, G. and Wahren, J. (1998) Cholesterol homeostasis in human brain: turnover of 24S-hydroxycholesterol and evidence for a cerebral origin of most of this oxysterol in the circulation. *J Lipid Res* **39**: 1594-1600.

Calpe-Berdiel, L., Rotllan, N., Fievet, C., Roig, R., Blanco-Vaca, F. and Escola-Gil, J. C. (2008) Liver X receptor-mediated activation of reverse cholesterol transport from macrophages to feces in vivo requires ABCG5/G8. *J Lipid Res* **49**: 1904-1911.

Cartagena, C. M., Ahmed, F., Burns, M. P., Pajoohesh-Ganji, A., Pak, D. T., Faden, A. I. and Rebeck, G. W. (2008) Cortical injury increases cholesterol 24S hydroxylase (Cyp46) levels in the rat brain. *J Neurotrauma* **25**: 1087-1098.

Chen, W., Chen, G., Head, D. L., Mangelsdorf, D. J. and Russell, D. W. (2007) Enzymatic reduction of oxysterols impairs LXR signaling in cultured cells and the livers of mice. *Cell Metab* **5**: 73-79.

Chen, J. Y., Levy-Wilson, B., Goodart, S. and Cooper, A. D. (2002) Mice expressing the human CYP7A1 gene in the mouse CYP7A1 knock-out background lack induction of CYP7A1 expression by cholesterol feeding and have increased hypercholesterolemia when fed a high fat diet. *J Biol Chem* **277**: 42588-42595.

Duanmu, Z., Weckle, A., Koukouritaki, S. B., Hines, R. N., Falany, J. L., Falany, C. N., Kocarek, T. A. and Runge-Morris, M. (2006) Developmental expression of aryl, estrogen, and hydroxysteroid sulfotransferases in pre- and postnatal human liver. *J Pharmacol Exp Ther* **316**: 1310-1317.

Dumas, N. A., He, D., Frost, A. R. and Falany, C. N. (2008) Sulfotransferase 2B1b in human breast: differences in subcellular localization in African American and Caucasian women. *J Steroid Biochem Mol Biol* **111**: 171-177.

Falany, C. N. (1997) Enzymology of human cytosolic sulfotransferases. *Faseb J* **11**: 206-216.

Falany, J. L. and Falany, C. N. (2007) Interactions of the human cytosolic sulfotransferases and steroid sulfatase in the metabolism of tibolone and raloxifene. *J Steroid Biochem Mol Biol* **107**: 202-210.

Falany, C. N., Krasnykh, V. and Falany, J. L. (1995) Bacterial expression and characterization of a cDNA for human liver estrogen sulfotransferase. *J Steroid Biochem Mol Biol* **52**: 529-539.

Falany, J. L., Macrina, N. and Falany, C. N. (2004) Sulfation of tibolone and tibolone metabolites by expressed human cytosolic sulfotransferases. *J Steroid Biochem Mol Biol* **88**: 383-391.

Falany, C. N., Comer, K. A., Dooley, T. P. and Glatt, H. (1995) Human dehydroepiandrosterone sulfotransferase. Purification, molecular cloning, and characterization. *Ann N Y Acad Sci* **774**: 59-72.

Falany, C. N., Wheeler, J., Oh, T. S. and Falany, J. L. (1994) Steroid sulfation by expressed human cytosolic sulfotransferases. *J Steroid Biochem Mol Biol* **48**: 369-375.

Falany, C. N., He, D., Dumas, N., Frost, A. R. and Falany, J. L. (2006) Human cytosolic sulfotransferase 2B1: isoform expression, tissue specificity and subcellular localization. *J Steroid Biochem Mol Biol* **102**: 214-221.

Fuda, H., Javitt, N. B., Mitamura, K., Ikegawa, S. and Strott, C. A. (2007) Oxysterols are substrates for cholesterol sulfotransferase. *J Lipid Res* **48**: 1343-1352.

Fujiyoshi, M., Ohtsuki, S., Hori, S., Tachikawa, M. and Terasaki, T. (2007) 24S-hydroxycholesterol induces cholesterol release from choroid plexus epithelial cells in an apical- and apoE isoform-dependent manner concomitantly with the induction of ABCA1 and ABCG1 expression. *J Neurochem* **100**: 968-978.

Geese, W. J. and Raftogianis, R. B. (2001) Biochemical characterization and tissue distribution of human SULT2B1. *Biochem Biophys Res Commun* **288**: 280-289.

Glatt, H., Engelke, C. E., Pabel, U., Teubner, W., Jones, A. L., Coughtrie, M. W., Andrae, U., Falany, C. N. and Meinl, W. (2000) Sulfotransferases: genetics and role in toxicology. *Toxicol Lett* **112-113**: 341-348.

Hernandez-Guzman, F. G., Higashiyama, T., Osawa, Y. and Ghosh, D. (2001) Purification, characterization and crystallization of human placental estrone/dehydroepiandrosterone sulfatase, a membrane-bound enzyme of the endoplasmic reticulum. *J Steroid Biochem Mol Biol* **78**: 441-450.

Huey, R., Morris, G. M., Olson, A. J. and Goodsell, D. S. (2007) A Semiemperical Free Energy Force Field with Charge-Based Desovation. *J Comput Chem* **28**: 1145-1152.

Iwamori, M. (2005) Estrogen sulfatase. *Methods Enzymol* **400**: 293-302.

Janowski, B. A., Grogan, M. J., Jones, S. A., Wisely, G. B., Kliewer, S. A., Corey, E. J. and Mangelsdorf, D. J. (1999) Structural requirements of ligands for the oxysterol liver X receptors

LXRalpha and LXRbeta. Proc Natl Acad Sci U S A **96**, 266-271.

Javitt, N. B., Lee, Y. C., Shimizu, C., Fuda, H. and Strott, C. A. (2001) Cholesterol and hydroxycholesterol sulfotransferases: identification, distinction from dehydroepiandrosterone sulfotransferase, and differential tissue expression. *Endocrinology* **142**: 2978-2984.

Jiang, Y. J., Kim, P., Elias, P. M. and Feingold, K. R. (2005) LXR and PPAR activators stimulate cholesterol sulfotransferase type 2 isoform 1b in human keratinocytes. *J Lipid Res* **46**: 57-66.

Kotov, A., Falany, J. L., Wang, J. and Falany, C. N. (1999) Regulation of estrogen activity by sulfation in human Ishikawa endometrial adenocarcinoma cells. *J Steroid Biochem Mol Biol* **68**: 137-144.

Koudinov, A. R. and Koudinova, N. V. (2002) Cholesterol's role in synapse formation. *Science* **295**: 2213.

Lascombe, M. B., Ponchet, M., Venard, P., Milat, M. L., Blein, J. P. and Prange, T. (2002) The 1.45 A resolution structure of the cryptogein-cholesterol complex: a close-up view of a sterol carrier protein (SCP) active site. *Acta Crystallogr D Biol Crystallogr* **58**: 1442-1447.

Lehmann, J. M., Kliewer, S. A., Moore, L. B., Smith-Oliver, T. A., Oliver, B. B., Su, J. L., Sundseth, S. S., Winegar, D. A., Blanchard, D. E., Spencer, T. A. and Willson, T. M. (1997) Activation of the nuclear receptor LXR by oxysterols defines a new hormone response pathway. *J Biol Chem* **272**: 3137-31340

Mast, N., Norcross, R., Andersson, U., Shou, M., Nakayama, K., Bjorkhem, I. and Pikuleva, I. A. (2003) Broad substrate specificity of human cytochrome P450 46A1 which initiates cholesterol degradation in the brain. *Biochemistry* **42**: 14284-14292.

Meloche, C. A. and Falany, C. N. (2001) Expression and characterization of the human 3 beta-hydroxysteroid sulfotransferases (SULT2B1a and SULT2B1b). *J Steroid Biochem Mol Biol* **77**: 261-269.

Naik, S. U., Wang, X., Da Silva, J. S., Jaye, M., Macphee, C. H., Reilly, M. P., Billheimer, J. T.,

Pedersen, L. C., Petrotchenko, E. V. and Negishi, M. (2000) Crystal structure of SULT2A3, human hydroxysteroid sulfotransferase. *FEBS Lett* **475**: 61-64.

Petrotchenko, E. V., Pedersen, L. C., Borchers, C. H., Tomer, K. B. and Negishi, M. (2001) The dimerization motif of cytosolic sulfotransferases. *FEBS Lett* **490**: 39-43.

Rehse, P. H., Zhou, M. and Lin, S. X. (2002) Crystal structure of human dehydroepiandrosterone sulphotransferase in complex with substrate. *Biochem J* **364**: 165-167.

Rothblat, G. H. and Rader, D. J. (2006) Pharmacological activation of liver X receptors promotes reverse cholesterol transport in vivo. *Circulation* **113**: 90-97.

Zhang, H., Varlamova, O., Vargas, F. M., Falany, C. N., Leyh, T. S. and Varmalova, O. (1998) Sulfuryl transfer: the catalytic mechanism of human estrogen sulfotransferase*. J Biol Chem* **273**: 10888-10892

Zhou, M., Rehse, P., Chang, H. J., Luu-The, V. and Lin, S. X. (2001) Crystallization and preliminary crystallographic results of apo and complex forms of human dehydroepiandrosterone sulfotransferase. *Acta Crystallogr D Biol Crystallogr* **57**: 1630-1633.

FOOTNOTE

This research was supported by NIH grants to CNF [GM38953], to MRM [ES/CA05823], to TAK [HL050710, and an Environmental Health Sciences Center Grant [ES06636] to Wayne State University.

FIGURE LEGENDS

Figure 1. Sulfated products of 24-OHChol generated by SULT2A1 and SULT2B1b, and sensitivity to hydrolysis by STS. A. The structure of 24-OHChol is shown and the arrows identify the 3-and 24-hydroxyl groups that are sulfated. B. The formation of 24-OHChol monosulfate and disulfate is shown as well as their sensitivity to STS hydrolysis. 24-OHChol (20 μM) was incubated with SULT2A1 or SULT2B1b in the presence of 10 μM [^{35}S]PAPS for 30 min at 37°C. The reactions were terminated by extraction with chloroform and an aliquot was applied to a silica gel TLC plate. For treatment with STS, an aliquot of the reaction after chloroform extraction was incubated with 1 ug of STS for 30 min 37°C. The STS reaction was extracted with chloroform and an aliquot of the aqueous phase spotted on the TLC plate. The plates were developed as described in Methods and exposed to autoradiograph film to identify ^{35}S-containing bands. [^{35}S]PAPS does not move from the loading zone.

Figure 2. Sulfation of 24-OHChol by SULT2A1. Increasing concentrations of 24-OHChol were sulfated by SULT2A1 (2.6 ng) in the presence of 10 μM [^{35}S]PAPS. Reactions were run for 10 min at 37°C then terminated by extraction with chloroform. The aqueous phase of duplicate reactions were then treated with STS for 30 min and stopped by chloroform extraction. Aliquots of the reactions were loaded onto Silica gel TLC plates and developed as described in Methods. The plates were then exposed to autoradiograph film and the radioactive bands scraped into vials for scintillation counting. Panel A shows the formation of 24-OHChol monosulfate and disulfate at low 24-OHChol concentrations. Panel B shows the levels of 24-OHChol monosulfate and disulfate formation with increasing 24-OHChol concentrations as well as the residual 24-OHChol monosulfate present after STS treatment.

Figure 3. Sulfation of 24-OHChol by SULT1E1. Increasing concentrations of 24-OHChol were sulfated by SULT1E1 in the presence of 10 μM [^{35}S]PAPS. Reactions were run for 20 min at 37°C then terminated by extraction with chloroform. The aqueous phase of duplicate reactions were then treated with STS for 30 min and stopped by chloroform extraction. Aliquots of the reactions were loaded onto Silica gel TLC plates and developed as described in Methods. The levels of 24-OHChol monosulfate and disulfate formation with increasing 24-OHChol concentrations as well as the residual 24-OHChol monosulfate present after STS treatment are shown.

Figure 4. Formation of 24-OHChol-sulfate by SULT2B1b. Increasing concentrations of 24-OHChol were converted to a monosulfate by SULT2B1b in the presence of 10 μM [^{35}S]PAPS. Each point represents the mean of three assays ± standard deviation. The error bars are essentially contained within the data points.

Figure 5. LC-MS/MS analysis of the 24-OHChol sulfates formed by SULT2A1 and SULT2B1b. Panel A shows the monosulfated products generated by sulfation of 24-OHChol with SULT2A1. MS/MS analysis of the peaks identified the more abundant peak as the 3-sulfate (9.0 min) and the smaller peak (8.3 min) as the 24-sulfate. Panel B demonstrates that the 24-OHChol disulfate eluted at 7.3 min consistent with its more charged nature. Panel C shows that STS treatment of the disulfate generates only the STS-resistant 24-sulfate eluting at 8.3 min. Panel D demonstrates that sulfation of 24-OHChol with SULT2B1b results in the formation of only the 3-monosulfate.

Figure 6. Identification of 24-OHChole-24-sulfate by LC-MS/MS analysis. The site of sulfate conjugation in the putative 24-OHChol-24-sulfate was analyzed by LC-MS/MS following fragmentation with increasing energies as described in Methods. After fragmentation at 60 eV, the major ions detected were the parent ion 24-OHChol (481 Da), the sulfate moiety (96.9 Da) and a fragment derived from the A-ring containing the 3-OH (59.1 Da). The presence of the 3-OH indicates the sulfate is conjugated at the 24-position.

Figure 7. Conversion of the 24-OHChol monosulfates to the disulfate by SULT2A1. The two 24-OHChol monosulfates were synthesized as described in Methods and used in reactions to assay their conversion to 24-OHChol disulfate by SULT2A1. The reactions used non-radiolabeled monosulfates and [^{35}S]PAPS to monitor formation of the disulfate using the TLC assay described in Methods. Panel A shows the conversion of 24-OHChol-3-sulfate to the disulfate and panel B displays the sulfation of 24-OHChol-24-sulfate to the disulfate. The data represents three sets of reactions done in duplicate.

Figure 8. Molecular simulation of the orientation of the 24-OHChol monosulfates in the active site of SULT2A1. The two monosulfates of 24-OHChol were molecularly oriented into the active site of SULT2A1 (PDB file 1EFH) using the Autodock program to allow sulfonation of the free hydroxyl to allow disulfate formation. Panel A shows the orientation of 24-OHChol-3-sulfate in the substrate binding site in the SULT2A1 monomer. The binding free energy (BFE) is -3.5

Kcal/mol and the 24-hydroxyl group is close to Ser97 (3.5 Ang) and His99 (6.0 Ang). Panel B demonstrates that in the SULT2A1 monomer structure, 24-OHChol-24-sulfate does not readily bind in the pocket but prefers to bind to Lys138 and Ser80 in an apparent non-catalytic orientation. The BFE of the 24-OHChol-24-sulfate in this orientation is -10.0 Kcal/mol. Panel C shows the orientation of 24-OHChol-24-sulfate in the SULT2A1 dimer structure. In the SULT2A1 dimer structure, Glu73 from the other monomer inhibits access of the 24-sulfate to Lys138 and allows for docking in the active site in an apparent catalytically active conformation. The BFE is -7.9 Kcal/mol and the 3-hydroxyl group is 4 Ang from His99.

Figure 9. *In vitro* interactions of 24-OHChol sulfate metabolites with LXRα**.** The LanthaScreen TR-FRET LXRα co-activator assay was used to evaluate the abilities of 24-OHChol-3-sulfate and 24OHChol-24-sulfate to interact with LXRα, either as agonists (A) or antagonists (B). T0901317 and 24-OH-Chol were included as positive control LXRα agonists, and antagonist activities were determined in the presence of 100 nM T0901317. Binding curves were generated using Prism 5. The EC50s for T091317 and 24-OHChol were 0.030 uM and 1.99 uM, respectively, and there was no detectable activation for the sulfated metabolites. The IC50s of the sulfated metabolites were 0.149 uM for 24-OHChol-3 sulfate and 0.309 uM for 24-OHChol-24-sulfate.

DMD Fast Forward. Published on July 9, 2009 as DOI: 10.1124/dmd.108.025759
This article has not been copyedited and formatted. The final version may differ from this version.

TABLES

Table 1. Kinetic parameters for the sulfation of 24-OHChol by expressed SULT isoforms. The sulfation reactions were carried out as described in Methods. Kinetic parameters were calculated using the Enzyme Kinetics program. Vmax is expressed as µmoles sulfated product/min/nmol enzyme and Kcat is per min.

SULT	Substrate	Product	Km (µM)	Vmax (µmol/min/nmol)	Kcat (min^{-1})
2B1b	24-OHChol	3-Monosulfate	23.5	5113	218
1E1	24-OHChol	3-Monosulfate	0.9	50	55
1E1	24-OHChol	Disulfate	4.9	14	4
2A1	24-OHChol	3-Monosulfate	3.7	807	218
2A1	24-OHChol	Disulfate	1.5	199	133
2A1	24-OHChol 24-S	Disulfate	0.1	265	2410
2A1	24-OHChol 3-S	Disulfate	4.0	452	113

Fig. 1

A.

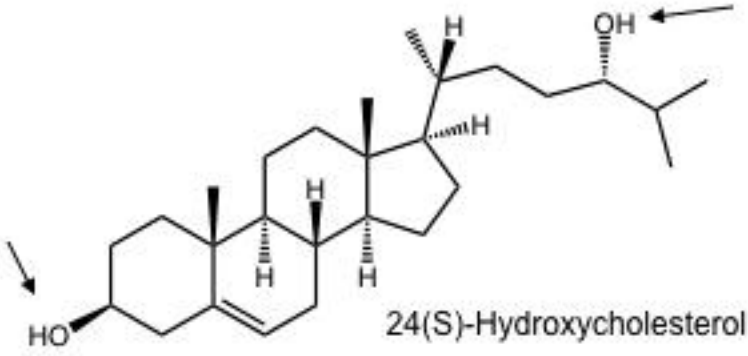

24(S)-Hydroxycholesterol

B.

Fig. 2

A.

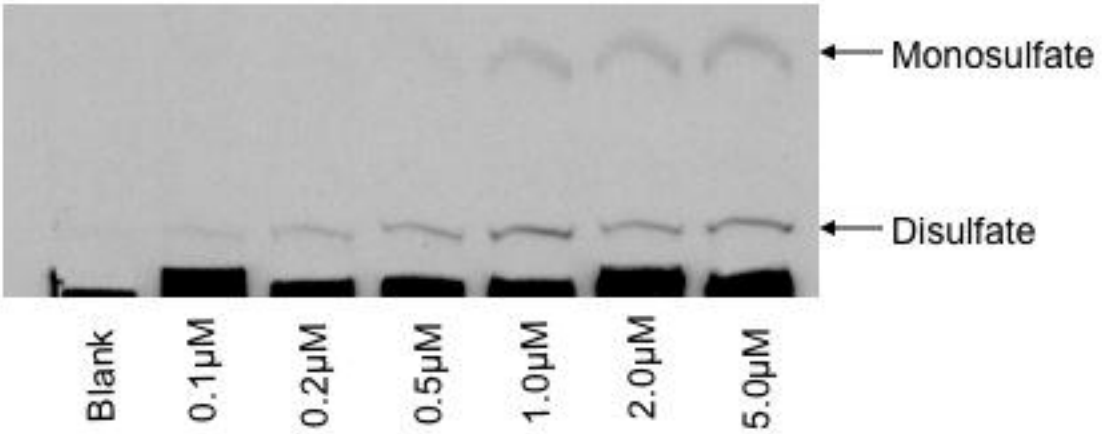
Monosulfate
Disulfate
Blank
0.1μM
0.2μM
0.5μM
1.0μM
2.0μM
5.0μM

B.

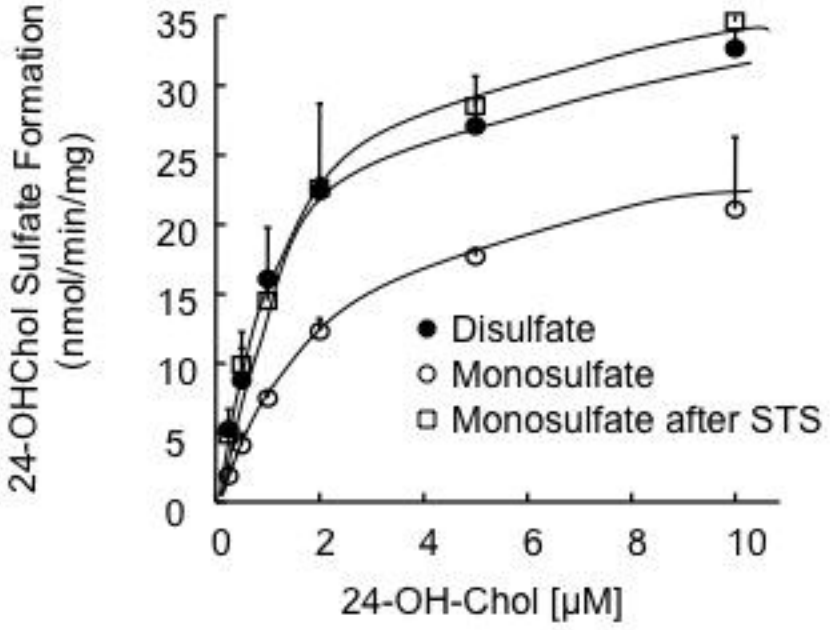
24-OHChol Sulfate Formation (nmol/min/mg)
35
30
25
20
15
10
5
0
0
2
4
6
8
10
24-OH-Chol [μM]
Disulfate
Monosulfate
Monosulfate after STS

Fig. 3

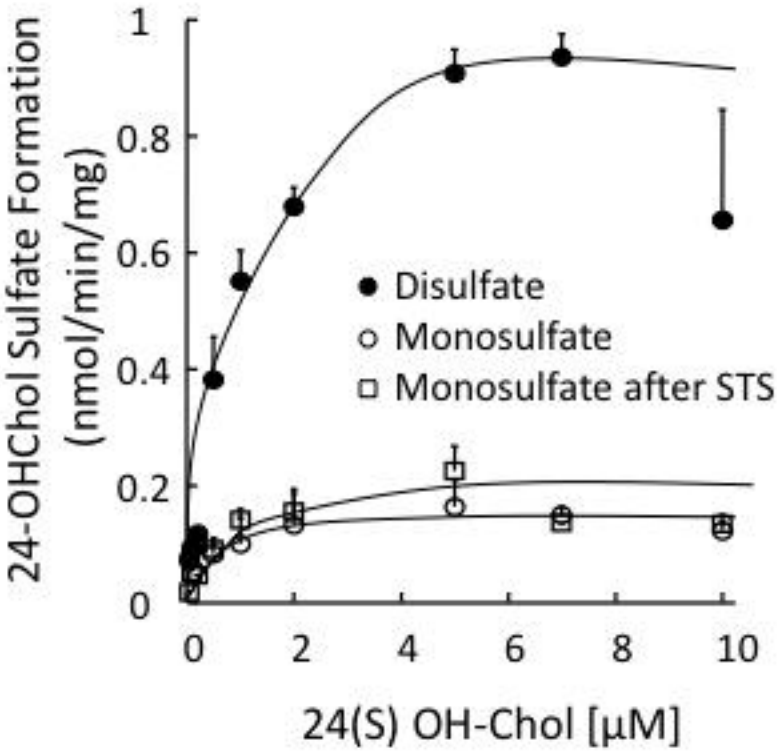
24-OHChol Sulfate Formation (nmol/min/mg)
1
0.8
0.6
0.4
0.2
0
0
2
4
6
8
10
24(S) OH-Chol [μM]
Disulfate
Monosulfate
Monosulfate after STS

Fig. 4

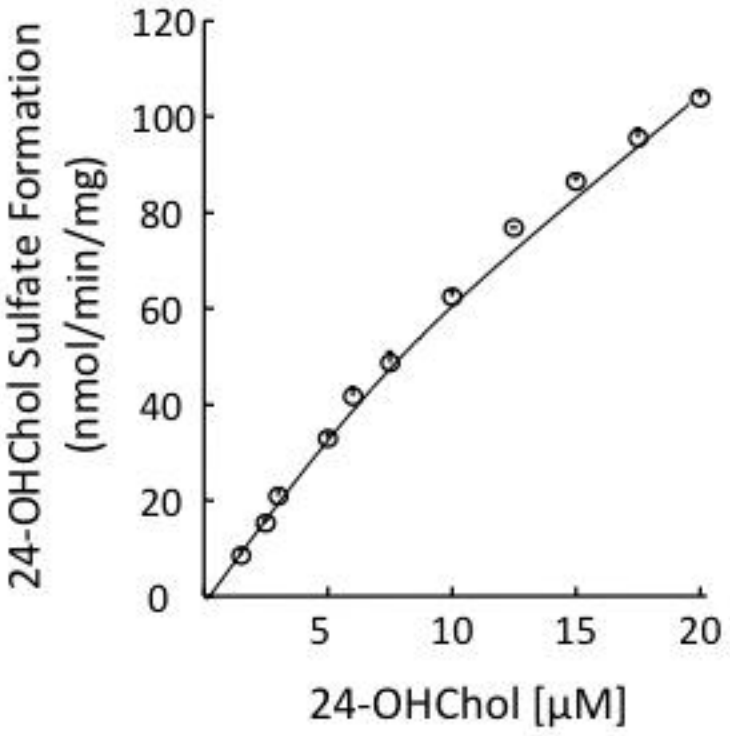
24-OHChol Sulfate Formation
(nmol/min/mg)
120
100
80
60
40
20
0
5
10
15
20
24-OHChol [μM]

Figure 5

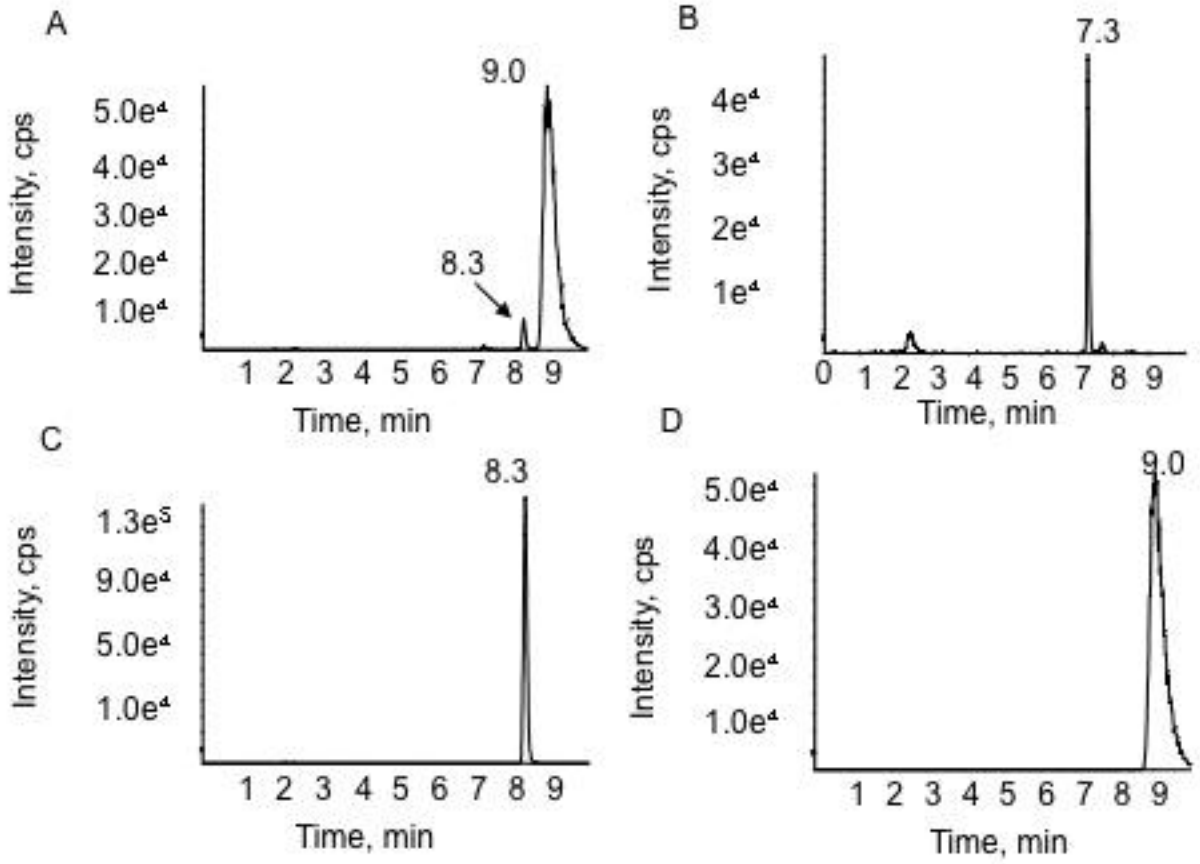
A
9.0
8.3
5.0e4
4.0e4
3.0e4
2.0e4
1.0e4
Intensity, cps
1 2 3 4 5 6 7 8 9
Time, min
B
7.3
4e4
3e4
2e4
1e4
Intensity, cps
0 1 2 3 4 5 6 7 8 9
Time, min
C
8.3
1.3e5
9.0e4
5.0e4
1.0e4
Intensity, cps
1 2 3 4 5 6 7 8 9
Time, min
D
9.0
5.0e4
4.0e4
3.0e4
2.0e4
1.0e4
Intensity, cps
1 2 3 4 5 6 7 8 9
Time, min

Fig. 6

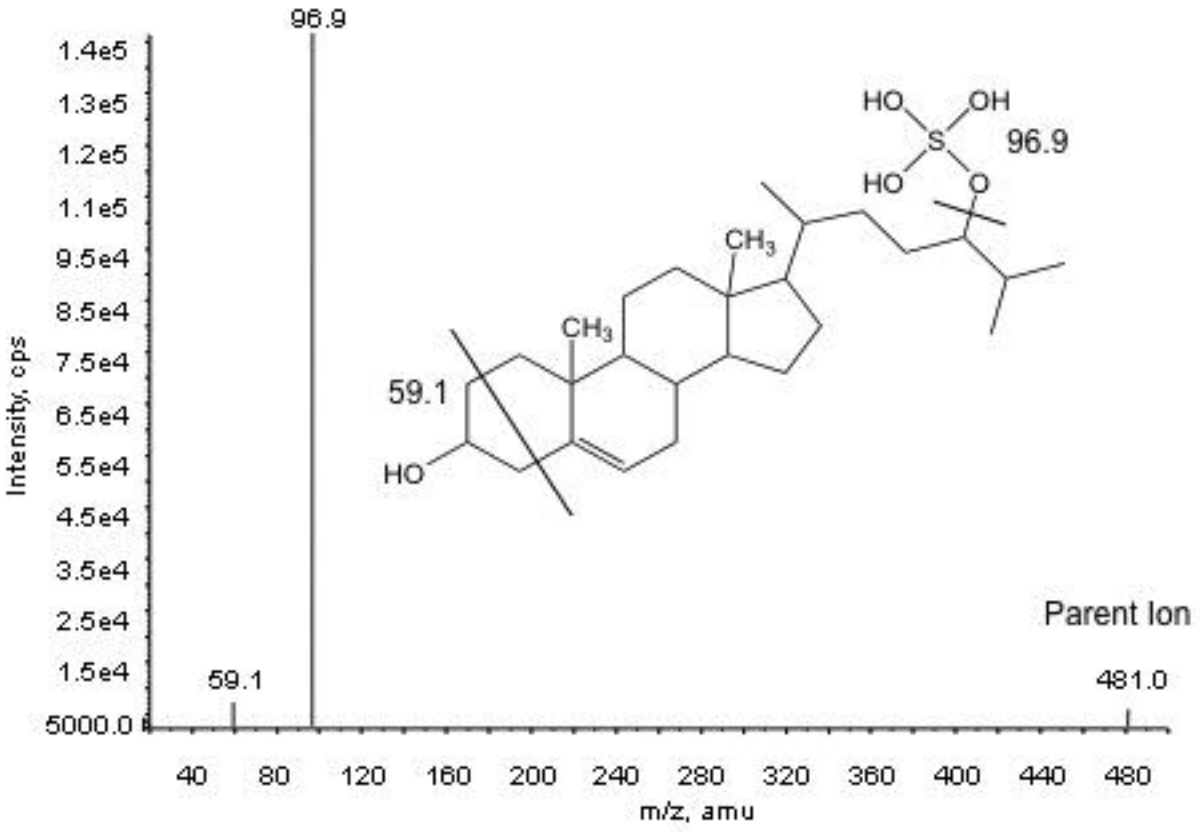
96.9
1.4e5
1.3e5
1.2e5
1.1e5
9.5e4
8.5e4
7.5e4
6.5e4
5.5e4
4.5e4
3.5e4
2.5e4
1.5e4
5000.0
Intensity, cps
59.1
481.0
Parent Ion
40
80
120
160
200
240
280
320
360
400
440
480
m/z, amu
HO
OH
S
O
96.9
CH3
CH3
59.1
HO

Fig. 7

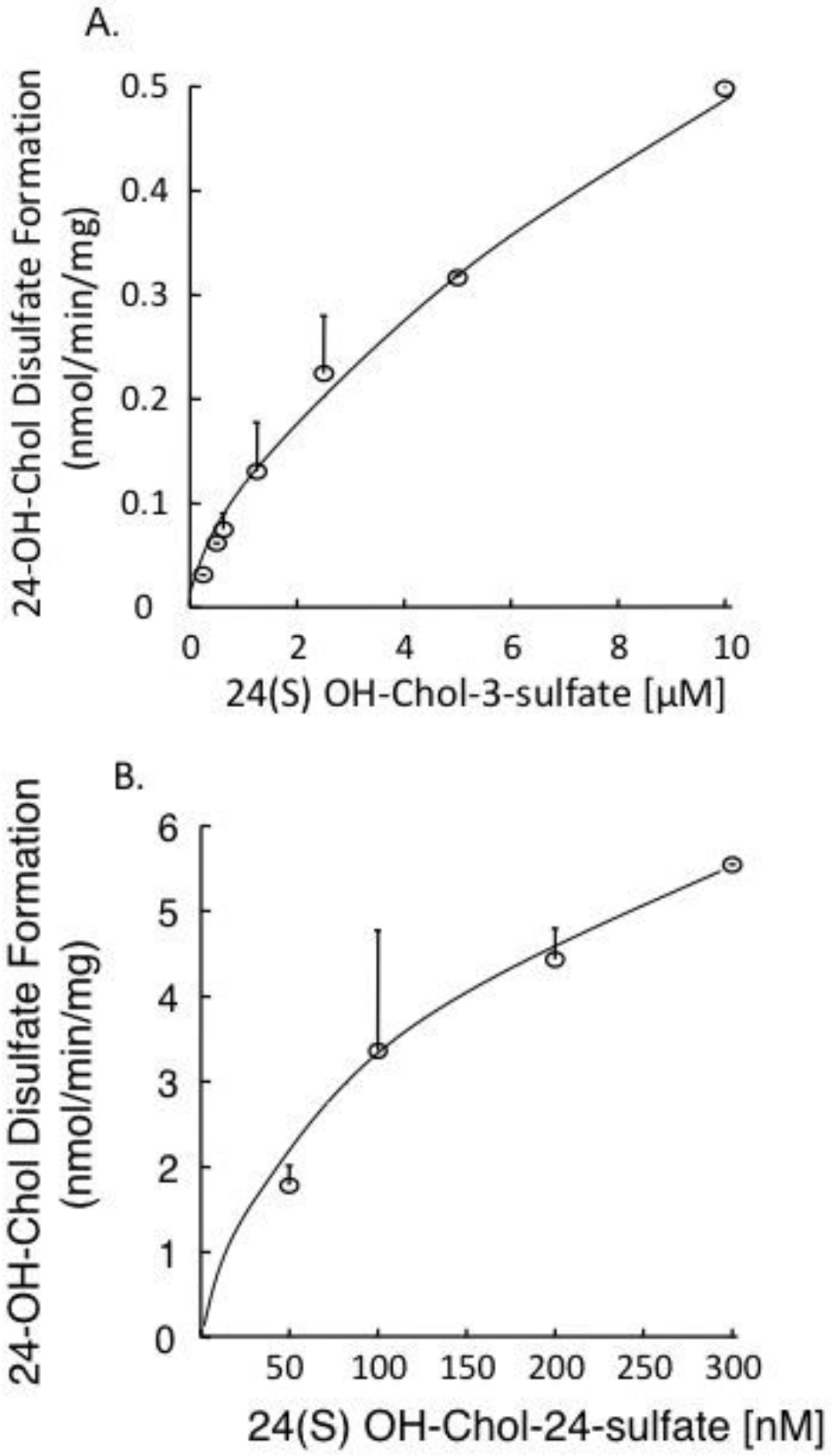
A.
24-OH-Chol Disulfate Formation (nmol/min/mg)
0.5
0.4
0.3
0.2
0.1
0
0
2
4
6
8
10
24(S) OH-Chol-3-sulfate [μM]
B.
24-OH-Chol Disulfate Formation (nmol/min/mg)
6
5
4
3
2
1
0
50
100
150
200
250
300
24(S) OH-Chol-24-sulfate [nM]

Figure 8

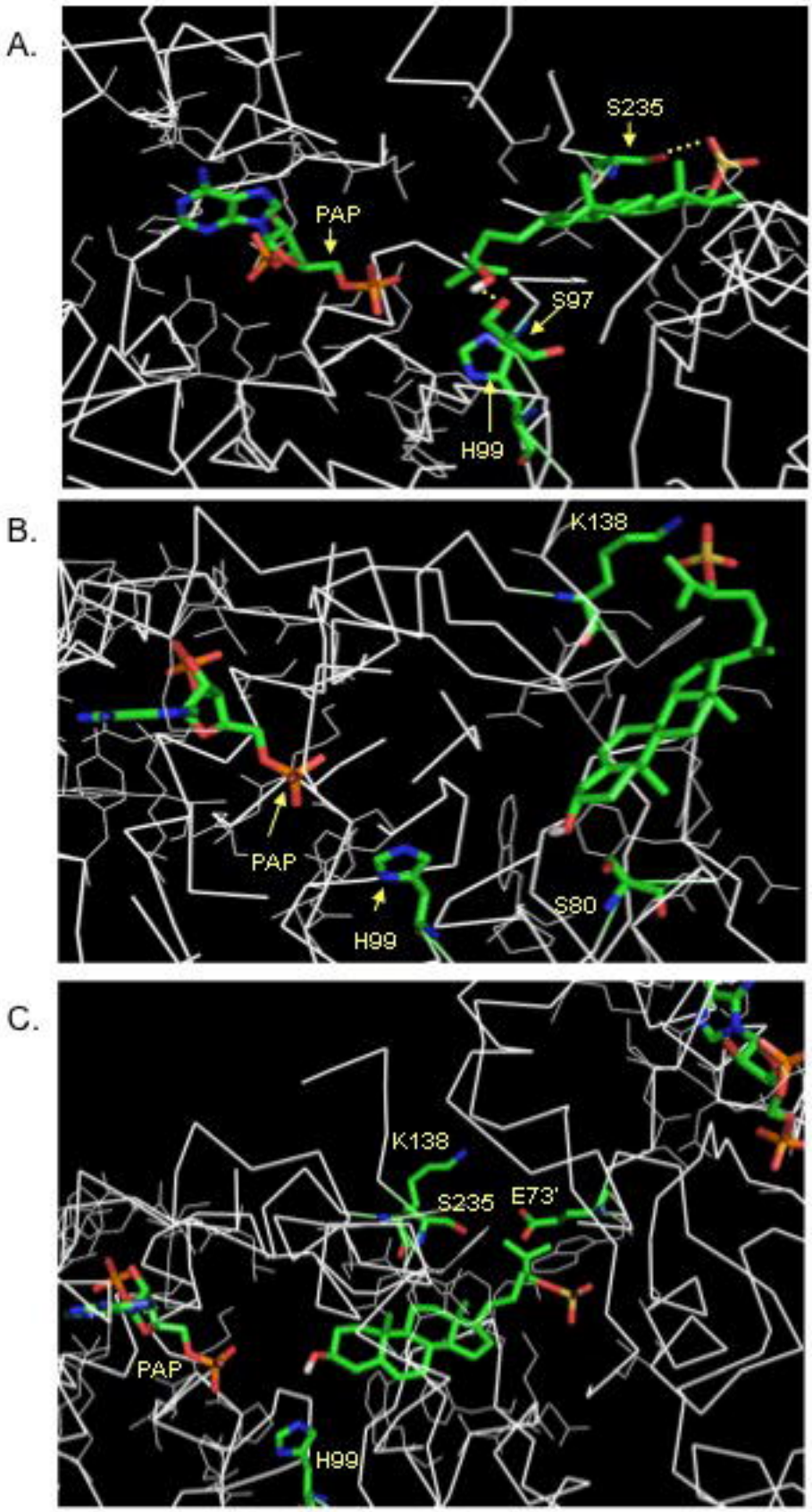

Figure 9

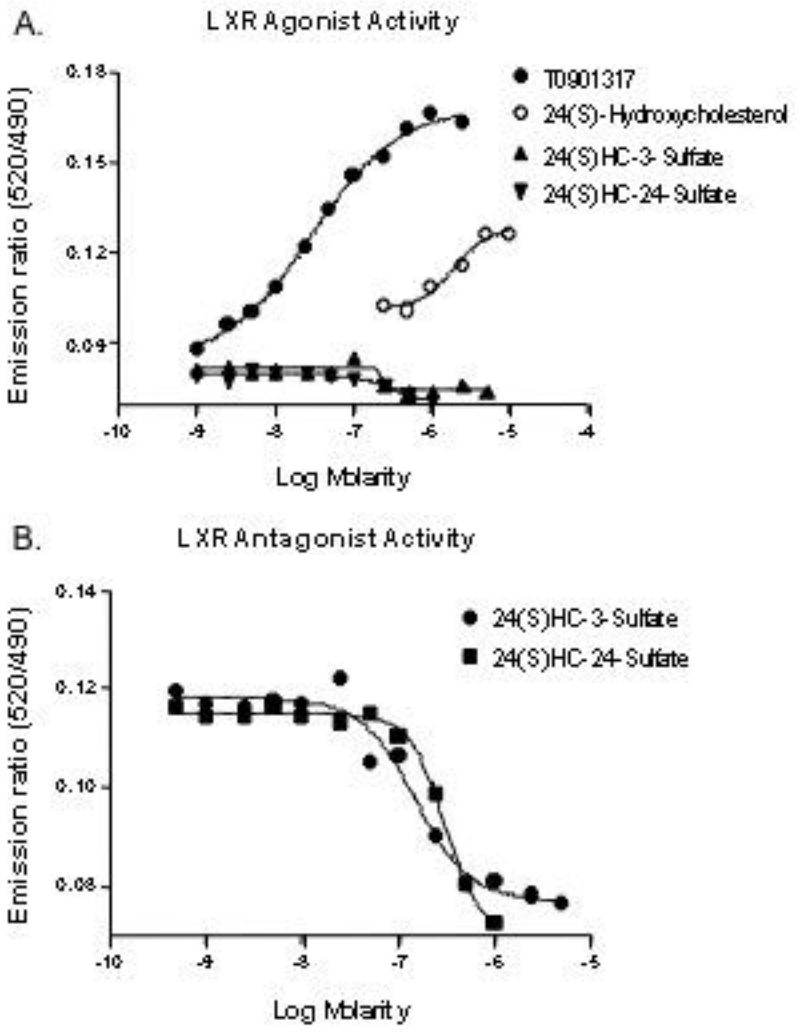
A.
LXR Agonist Activity
Emission ratio (520/490)
0.18
0.15
0.12
0.09
-10
-9
-8
-7
-6
-5
-4
Log Molarity
T0901317
24(S)-Hydroxycholesterol
24(S)HC-3-Sulfate
24(S)HC-24-Sulfate
B.
LXR Antagonist Activity
Emission ratio (520/490)
0.14
0.12
0.10
0.08
-10
-9
-8
-7
-6
-5
Log Molarity
24(S)HC-3-Sulfate
24(S)HC-24-Sulfate

Supplemental Figure 1. 24OHChol bound in the SULT2A1 monomer with the 3-OH oriented towards the PAP molecule. The first two orientations with the lowest BFE are shown. PAP is shown in yellow. 24OHChol is shown in magenta.

#1

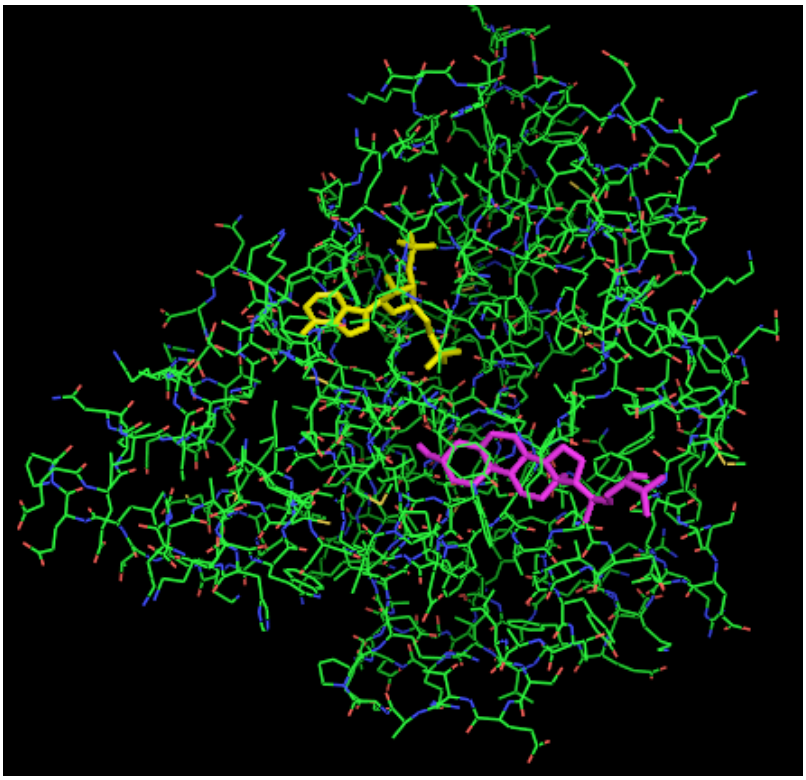

#2

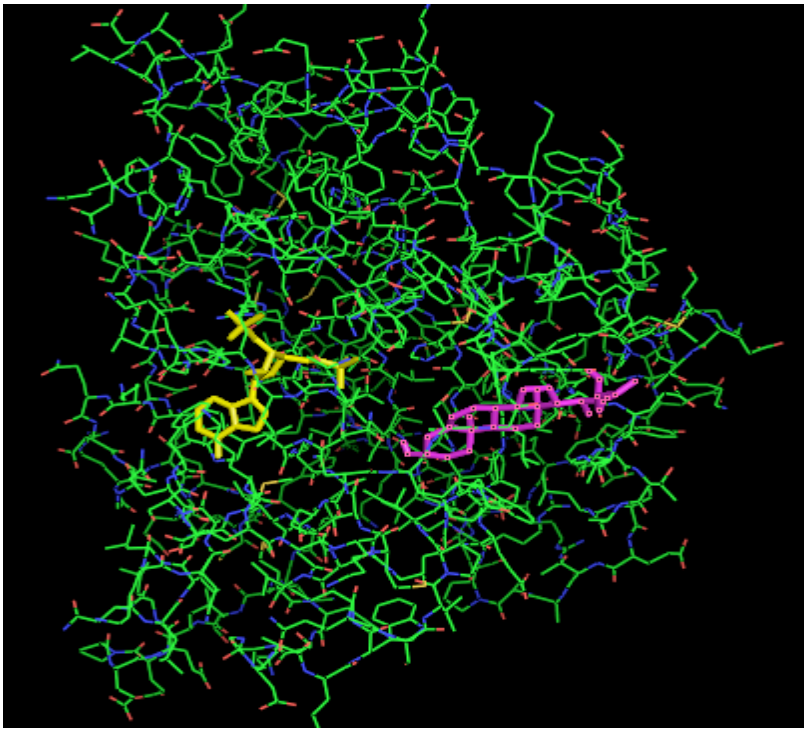

Supplemental Figure 2. 24OHChol bound in the SULT2A1 monomer with the 24-OH oriented towards the PAP molecule. The first two orientations with the lowest BFE are shown. PAP is shown in yellow. 24OHChol is shown in magenta.

#1

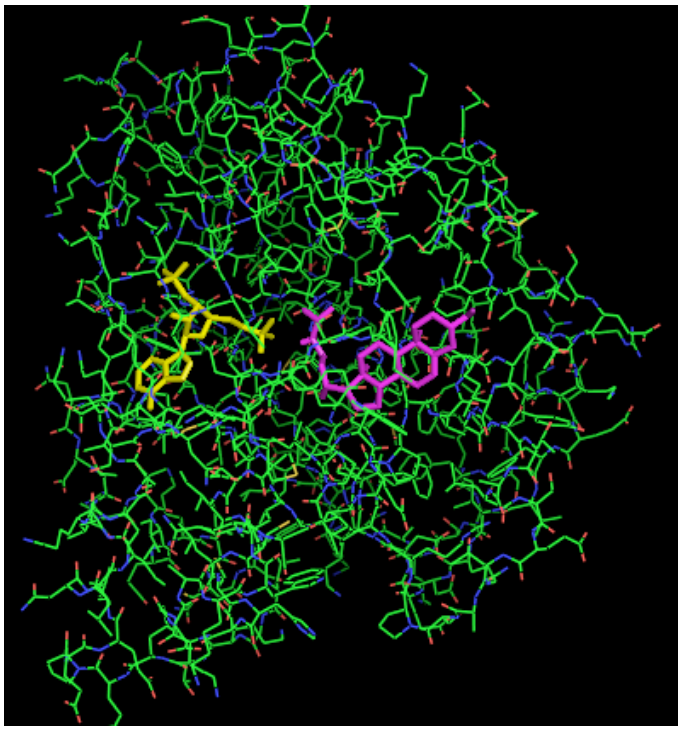

#2

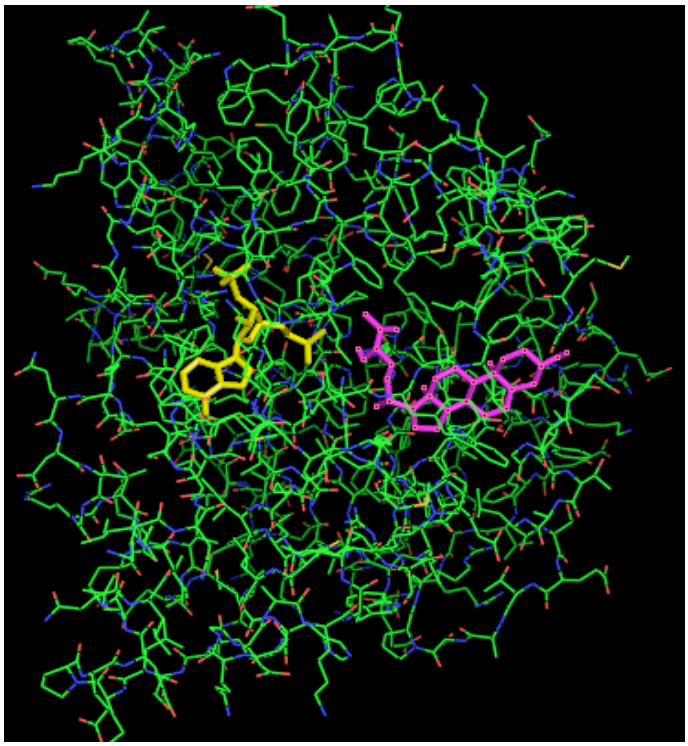

Supplemental Figure 3. 24OHChol-3-sulfate bound in the SULT2A1 monomer with the 24-OH oriented towards the PAP molecule. The second two orientations with the lowest BFE are shown. PAP is shown in yellow. 24OHChol is shown in magenta and the sulfonate is in cyan.

#2

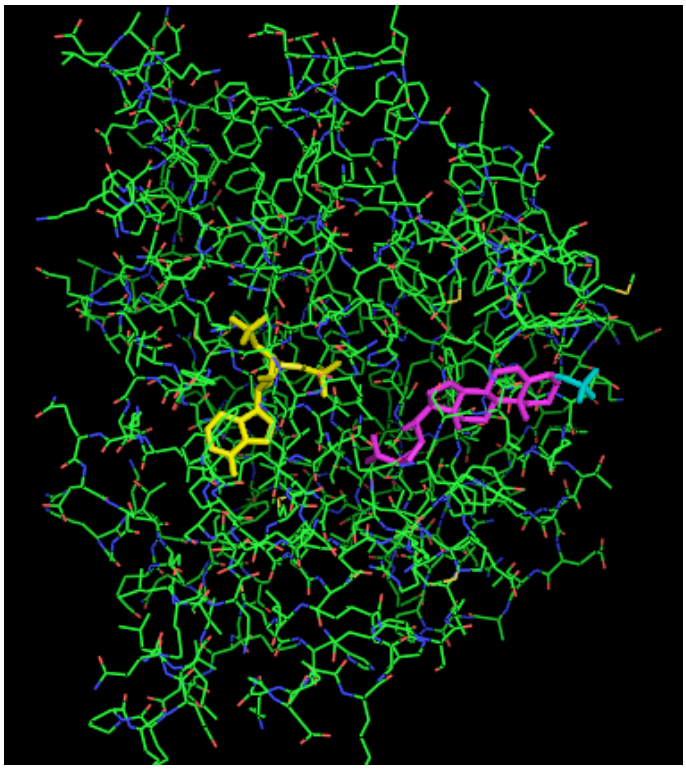

#3

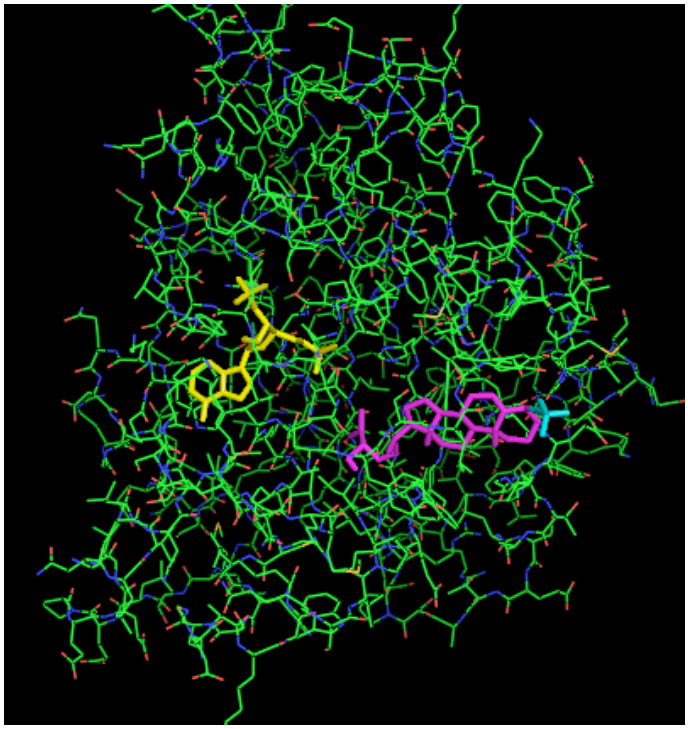

Supplemental Figure 4. 24OHChol-24-sulfate bound in the SULT2A1 monomer with the 3-OH oriented towards the PAP molecule. The second two orientations with the lowest BFE are shown. PAP is shown in yellow. 24OHChol is shown in magenta and the sulfonate is in cyan.

#2

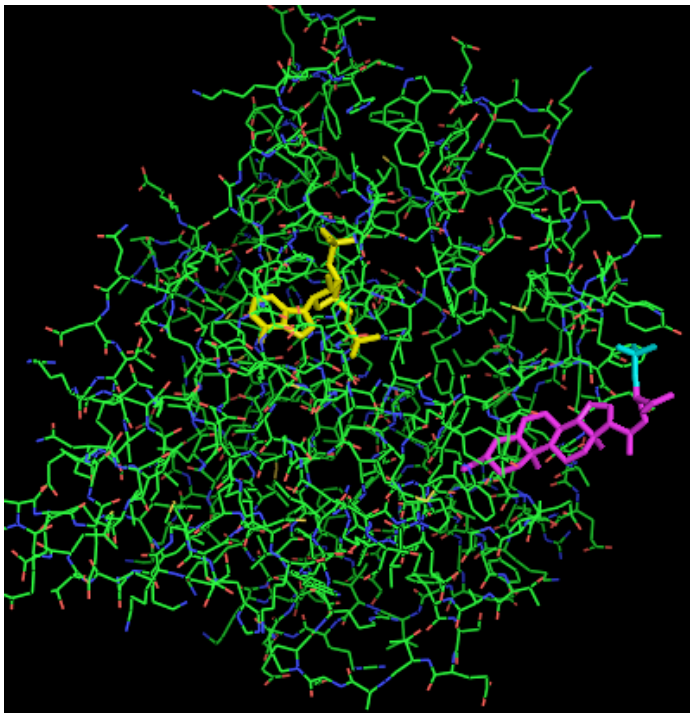

#3

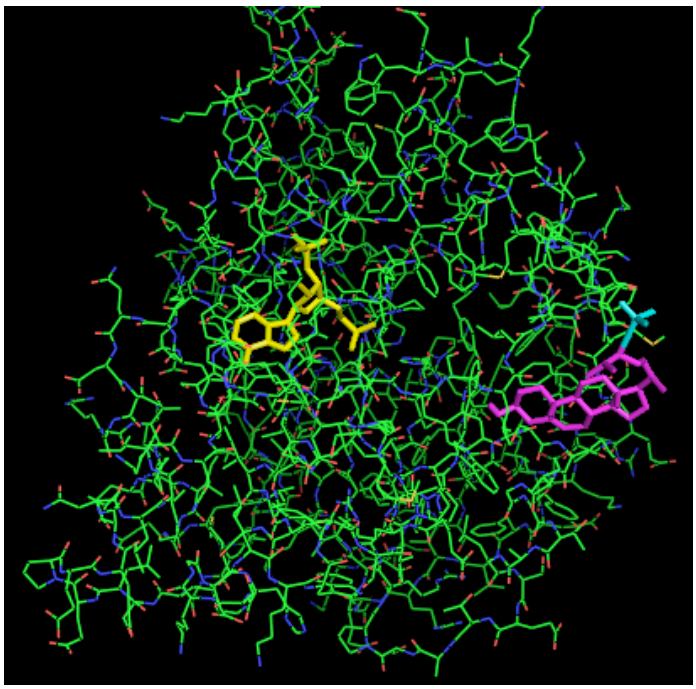

Supplemental Figure 5. 24OHChol-24-sulfate bound in the SULT2A1 dimer with the 3-OH oriented towards the PAP molecule. The second two orientations with the lowest BFE are shown. PAP is shown in yellow (note PAP molecule in each SULT2A1 monomer). 24OHChol is shown in magenta and the sulfonate is in cyan.

#2

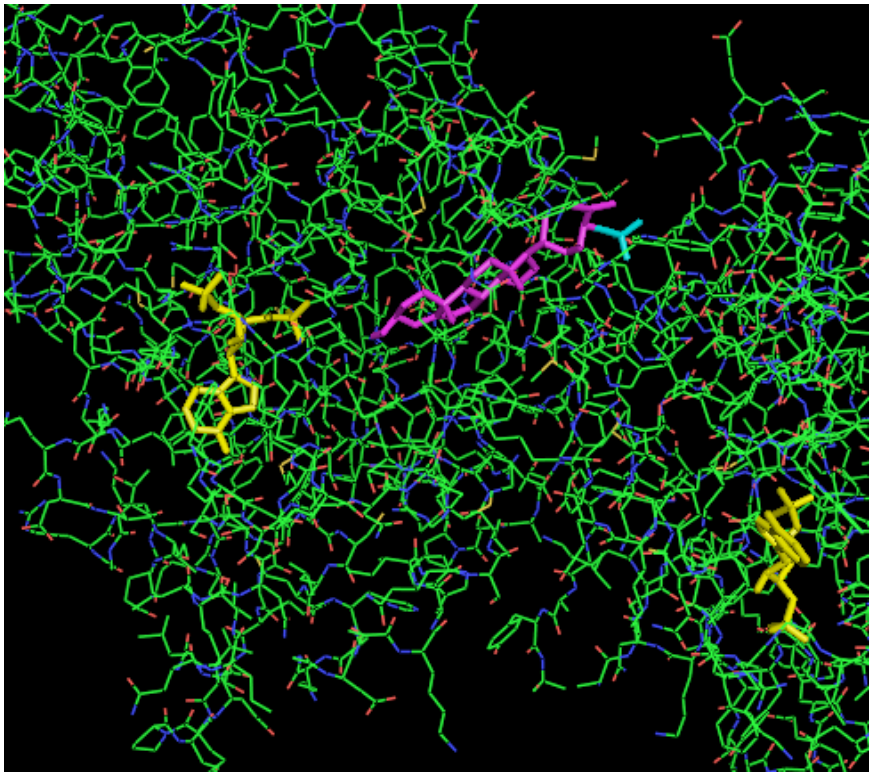

#3

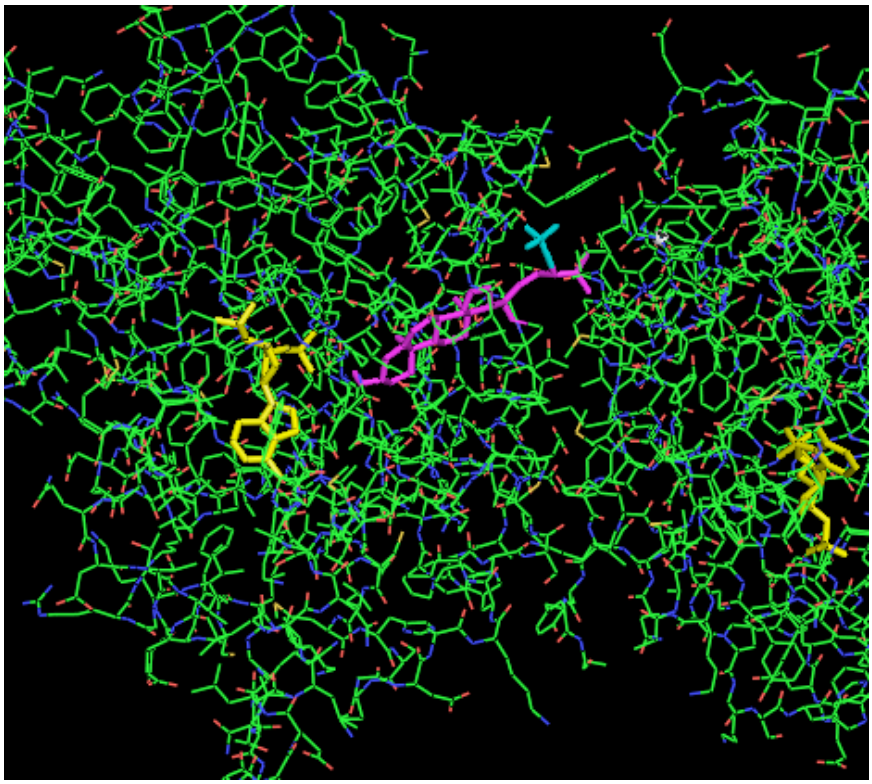

A.

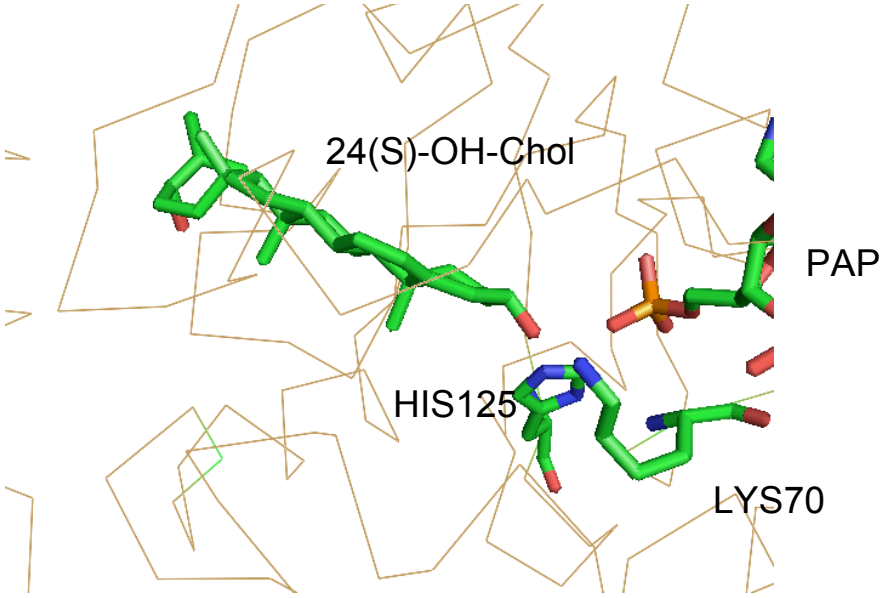

B.

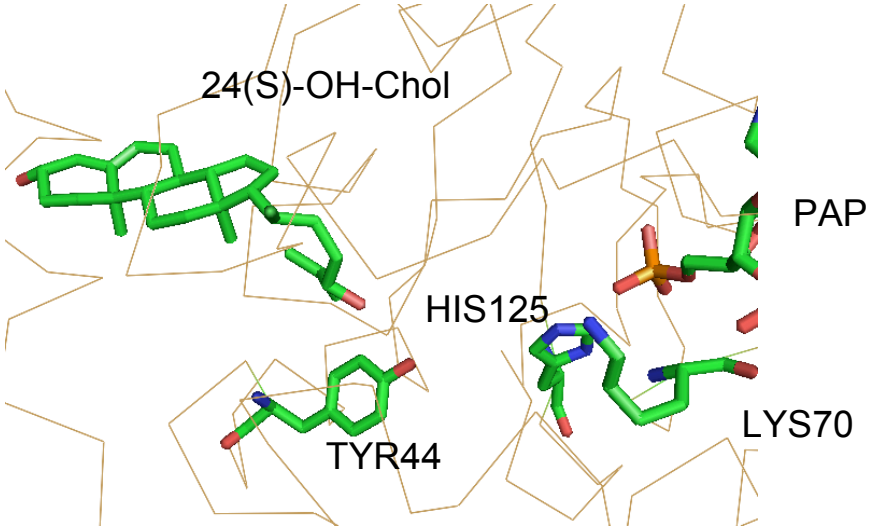

Supplemental Figure 6. Molecular docking of 24(S)-OHChol in the active site of SULT2B1b. Panel A represents the favoredorientation (BFE of -13.9kJ) with the 3-OH lacated 2.5 Ang from the active site His125 and PAP. This orientation is highly favorable for catalysis. Panel B displays the favored orientation when attempting to dock the 24-OH in the active site. The BFE for B was -11.4kJ, however the 24-OH is 8 Ang from the His125 and PAP in a position that is not catalytically favorable.